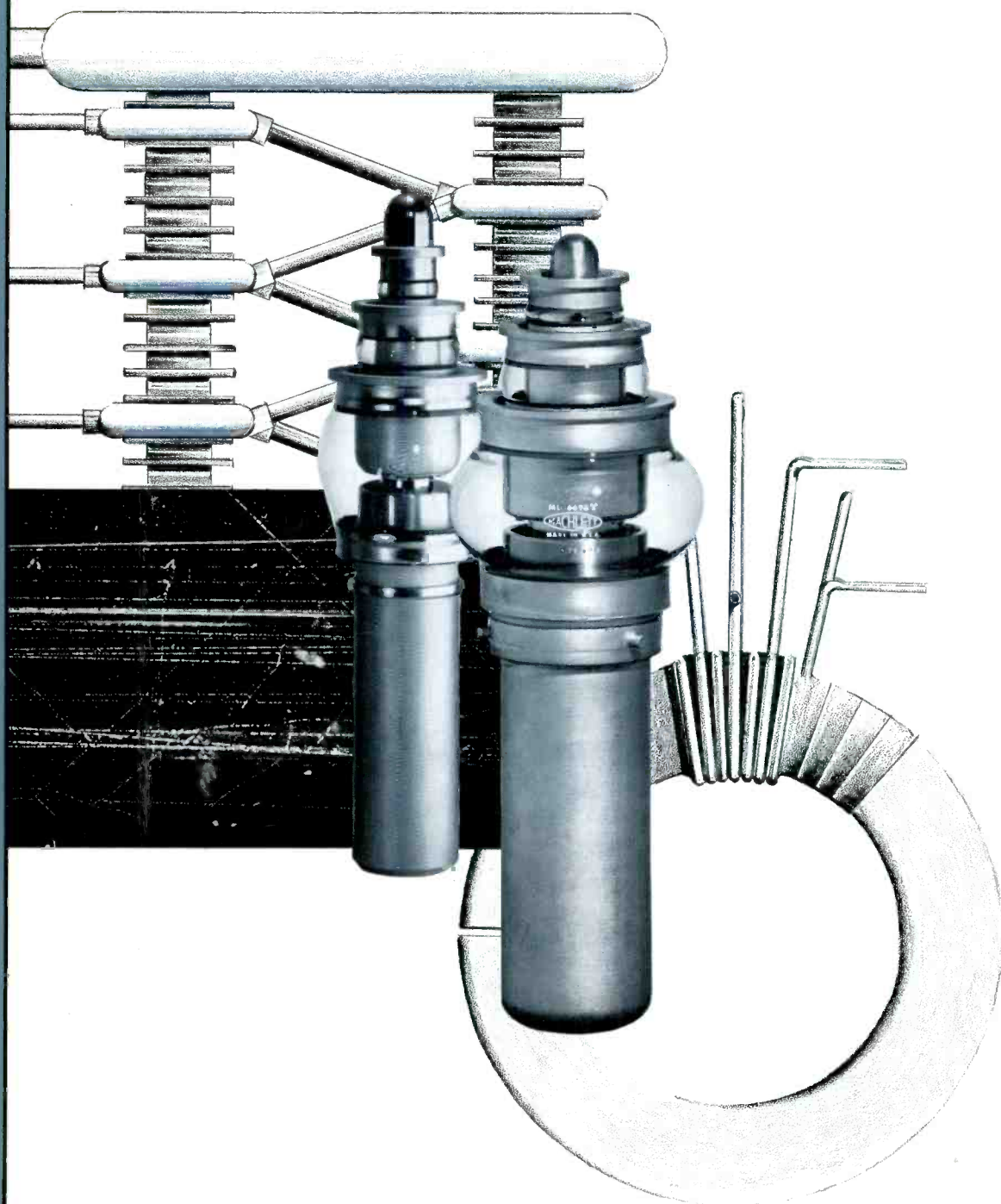


MACHLETT

CATHODE PRESS



VOL. 20 • NO. 2 • 1963

CATHODE PRESS

Vol. 20, No. 2, 1963

Editor, *Richard N. Rose*

Art Director, *Edward J. Bulger*

IN THIS ISSUE

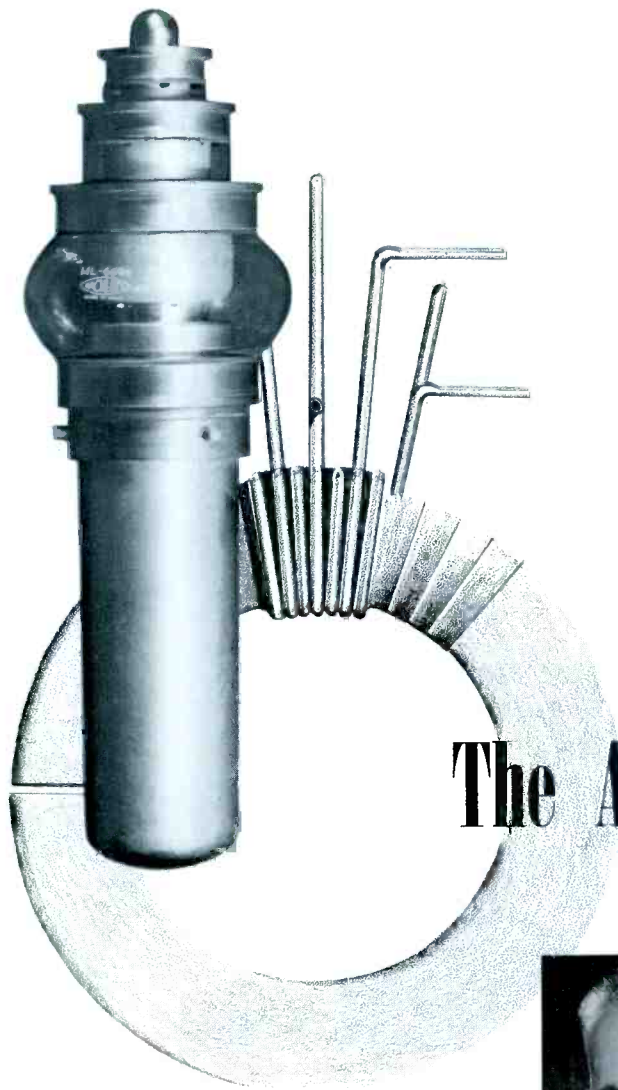
The Alternating Gradient Synchrotron and Machlett Power Tubes	2
Tube Life of ML-6421F vs. ML-5667 at Station WWV	19
The Impact of Space Environment on Electron Tube Design	20
Design of CW Amplitrons for Space Applications	26
Negative Grid Tubes for Space Applications	33
Notes on Vapor Cooling of High Power Electron Tubes	36
New Machlett Developments	43

COVER . . . is a representation of the subject of the initial article in this issue: The Alternating Gradient Synchrotron, a facility of the Brookhaven National Laboratory.

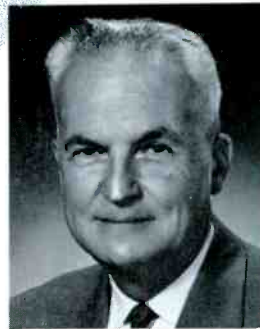
Published by:
The Machlett Laboratories, Inc.
An Affiliate of Raytheon Co.
Springdale, Connecticut

Product lines represented in this issue:

Large Power Tubes
Small Power Tubes
Photosensitive, Storage & Display Tubes



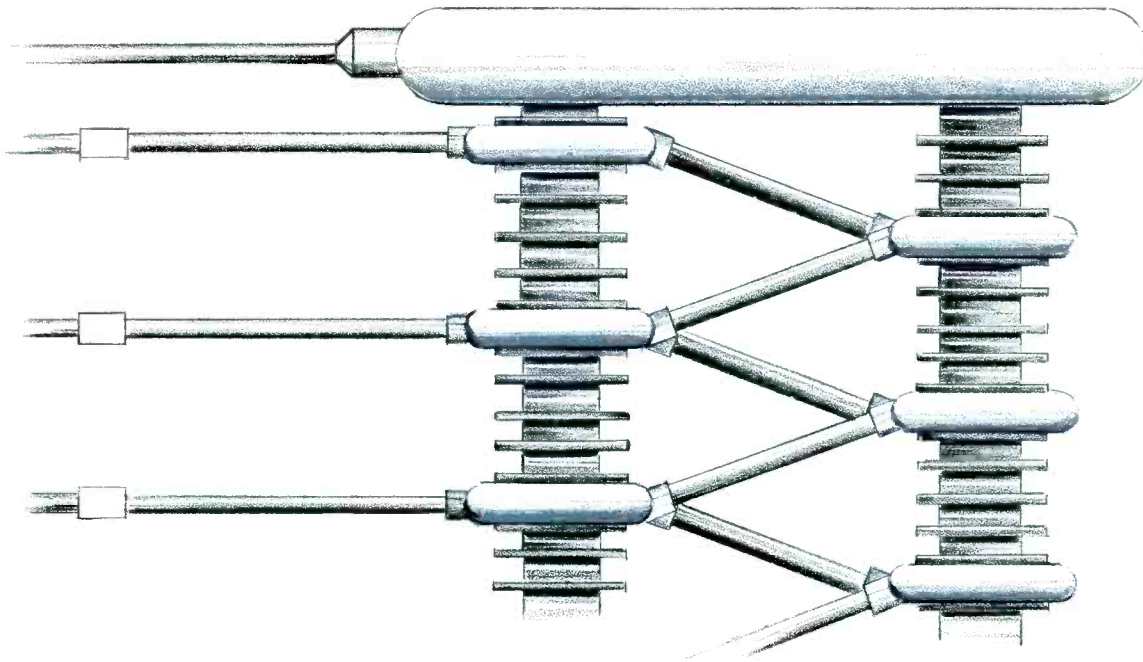
The Alternating Gradient



R. H. RHÉAUME

Raymond H. Rhéaume received the M.E. degree from Stevens Institute of Technology and the M.S. in E.E. degree from Columbia University. He is a senior member of the Institute of Electrical and Electronics Engineers, a licensed professional engineer in the states of New York and Connecticut, a member of the National Society of Professional Engineers, the New York State Society of Professional Engineers, and Tau Beta Pi. He is listed in "American Men of Science."

His professional connections have included Bell Telephone Laboratories, Western Electric Company, Machlett Laboratories, and Hanovia Chemical and Manufacturing Co., Electrical Division. He is now an electrical engineer on the scientific staff of the Brookhaven National Laboratory.



Synchrotron and Machlett Power Tubes*

By R. H. RHÉAUME, *Brookhaven National Laboratory
Associated Universities, Inc.
Upton, L. I., N. Y.*

In the ferrite-coupled wideband power amplifier stages of the Brookhaven Alternating Gradient Synchrotron, ML-6424 and ML-6696 coaxial triodes help accelerate protons to an energy of 33 billion electron volts.

Introduction

From the early days of x-rays there has been a Machlett tradition of service to atomic science and technology through contributions to the art of high vacuum tubes¹. Modern super-energy particle accelerators are themselves very large high vacuum tubes designed for studying subatomic particles, the building blocks of the universe. The most important of these high energy physics research machines, the cyclic particle accelerators, rely upon high-power electron tubes for radio frequency accelerating energy. The largest accelerator yet

to be built, the Brookhaven Alternating Gradient Synchrotron, requires not only more, but also more precisely controlled rf accelerating power than former machines, and employs ML-6424 and ML-6696 coaxial power triodes toward this purpose.

Brookhaven and the AGS

Studies of atomic nuclei form a major part of the research program of Brookhaven National Laboratory, a national center for fundamental and applied research in the nuclear sciences and related subjects situated at Upton, Long Island, New York. This research, which is basic to nuclear science, broadly involves all the major machines and ranges from measurements of the masses and other properties of undisturbed nuclei to observations of the violent disruptions resulting from nuclear fission and from bombardment of targets by ultra-high energy particles. Workers in this field use accelerators of various designs at many different energy levels, since the experimental results vary with the energies of the bombarding particles. With the aid of the more recent machines, new particles such as mesons and hyperons have been discovered; the latest discovery has been the verification of the existence of two kinds of neutrinos and their corresponding anti-particles by means of the Alternating Gradient Synchrotron, or AGS. A summary of known fundamental particles and interactions is presented in Table I.

*Work carried out under contract with U. S. Atomic Energy Commission.

¹Machlett Cathode Press, Memorial Issue, 1955.

TABLE 1 Fundamental

CLASS	NAME	PARTICLES			ANTI-PARTICLES		
		S = -2			S = +2		
BARYONS STRONGLY INTERACTING FERMIONS (SPIN = 1/2 ħ)	CASCADE HYPERON ISOTOPIC SPIN T = 1/2	Ξ^0 Ξ^-			Ξ^+ Ξ^0		
	SIGMA HYPERON T = 1	Σ^+ $T_3 = +1$	Σ^0 $T_3 = 0$	Σ^- $T_3 = -1$	Σ^+ $T_3 = +1$	Σ^0 $T_3 = 0$	Σ^- $T_3 = -1$
	LAMBDA HYPERON T = 0	Λ^0			$\bar{\Lambda}^0$		
	NUCLEON (PROTON-NEUTRON) T = 1/2	p^+ $T_3 = +1/2$	n^0 $T_3 = -1/2$	BARYON CHARGE CENTER	\bar{n}^0 $T_3 = +1/2$	\bar{p}^- $T_3 = -1/2$	ANTI-BARYON CHARGE CENTER
MESONS STRONGLY INTERACTING BOSONS (SPIN = 0)	K MESON T = 1/2	K^+ $T_3 = +1/2$	K^0 $T_3 = -1/2$	HEAVY MESON CHARGE CENTER \downarrow	K^0 $T_3 = +1/2$	K^- $T_3 = -1/2$	
	PI MESON T = 1	π^+ $T_3 = +1$	π^0 $T_3 = 0$	π^- $T_3 = -1$	π^0 $T_3 = +1$	π^- $T_3 = -1$	
	LEPTONS WEAKLY INTERACTING FERMIONS (SPIN = 1/2 ħ)	MUON μ^-	μ^+	ELECTRON e^-	e^+ (POSITRON)	NEUTRINO ν	$\bar{\nu}$
MASSLESS BOSONS (SPIN = 1 ħ) (SPIN = 2 ħ)	PHOTON γ	GRAVITON ?					

Particles & Interactions

REST MASS IN Mev		MEAN LIFE IN SECONDS	DECAY SCHEMES
Ξ^{\pm}	≈ 1320	1.3×10^{-10}	$\Xi^{\pm} \rightarrow \Lambda^0 + \pi^{\pm}$
Ξ^0	≈ 1310	1.5×10^{-10}	$\Xi^0 \rightarrow \Lambda^0 + \pi^0$
Σ	≈ 1190	0.8×10^{-10}	$\Sigma^+ \rightarrow \begin{cases} p^+ + \pi^0 & (50\%) \\ n^0 + \pi^+ & (50\%) \end{cases}$
		$< 10^{-12}$	$\Sigma^0 \rightarrow \Lambda^0 + \gamma$
		1.7×10^{-10}	$\Sigma^- \rightarrow n^0 + \pi^-$
Λ^0	1115	2.5×10^{-10}	$\Lambda^0 \rightarrow \begin{cases} p^+ + \pi^- & (67\%) \\ n^0 + \pi^0 & (33\%) \end{cases}$
n	939.5	1.01×10^3	$n^0 \rightarrow p^+ + e^- + \bar{\nu}$
p	938.2	STABLE	
K^+	494	1.2×10^{-8}	$\rightarrow \pi^0 + e^+ + \nu$ (5%)
			$\rightarrow \pi^0 + \mu^+ + \nu$ (5%)
K_1^0	498	1×10^{-10}	$\rightarrow \mu^+ + \nu$ (64%)
			$\rightarrow \pi^+ + \pi^0$ (19%)
K_2^0	498	$\sim 6 \times 10^{-8}$	$\rightarrow 2\pi^+ + \pi^-$ (6%)
			$\rightarrow \pi^+ + 2\pi^0$ (2%)
K_1^0	498	$\sim 6 \times 10^{-8}$	$\rightarrow \pi^+ + \pi^-$ ($\approx 34\%$)
			$\rightarrow 2\pi^0$ ($\approx 16\%$)
K_2^0	498	$\sim 6 \times 10^{-8}$	$\rightarrow \pi^+ + \pi^- + \pi^0$ } (7%)
			$\rightarrow 3\pi^0$ }
K_2^0	498	$\sim 6 \times 10^{-8}$	$\rightarrow \pi^{\pm} + \mu^{\pm} + \bar{\nu}$ (19%)
			$\rightarrow \pi^{\pm} + e^{\pm} + \nu$ (24%)
π^-	140	2.6×10^{-8}	$\pi^- \rightarrow \mu^- + \bar{\nu}$
π^0	135	2.3×10^{-16}	$\pi^0 \rightarrow \gamma + \gamma$ ($\pi^0 \rightarrow \gamma + e^+ + e^-$ 1%)
π^+	140	2.6×10^{-8}	$\pi^+ \rightarrow \mu^+ + \nu$ ($\pi^+ \rightarrow e^+ + \nu$.01%)
	105.7	2.2×10^{-6}	$\mu^- \rightarrow e^- + \nu + \bar{\nu}$
	0.51	STABLE	
	0	The neutrinos associated with μ^{\pm} are different from those with e^{\pm}	
	0	STABLE	
	0	STABLE	NOT DETECTED

Table 1 continued — Fundamental Particles and Interactions

THE INTERACTIONS

<p>GRAVITY</p> <p>Gravitational "charge" is mass. Gravitational force between particles negligible. Force falls off with inverse square of distance-velocity independent -always attractive. Graviton - agent of force - not detected.</p>	<p>STRONG NUCLEAR</p> <p>Short range force. Charge independent. Strength of force when nucleons touch is over 100 times greater than electric force. Agent of force is π meson.</p>
<p>ELECTROMAGNETISM</p> <p>Charge - Q - quantized - either + or -. Agent of force is photon. E-M force responsible for atomic and molecular binding, hence for most "forces" of everyday world. Force is velocity dependent, changing aspect from electrostatic to electromagnetic depending on relative velocity of source and observer. Force can be attractive or repulsive.</p>	<p>WEAK INTERACTIONS</p> <p>10^{-13} times weaker than strong nuclear. Responsible for β-decay radioactivity and particle decays taking longer than 10^{-15} seconds</p>

THE RULES

<p>THE DESCRIPTION OF ALL INTERACTIONS</p> <table style="width: 100%; border: none;"> <tr> <td style="vertical-align: top;"> <p><i>Is independent of:</i></p> <p>Space translation Time translation Space rotation Zero of electric potential Inverse of space and charge together Reversal of time ?</p> </td> <td style="vertical-align: top;"> <p><i>Leading to conservation of:</i></p> <p>Momentum Energy-Mass Angular momentum Charge Product of space parity and charge reflection Time parity Baryons and leptons</p> </td> </tr> </table>	<p><i>Is independent of:</i></p> <p>Space translation Time translation Space rotation Zero of electric potential Inverse of space and charge together Reversal of time ?</p>	<p><i>Leading to conservation of:</i></p> <p>Momentum Energy-Mass Angular momentum Charge Product of space parity and charge reflection Time parity Baryons and leptons</p>	<p>THE STRONG AND ELECTROMAGNETIC (BUT NOT THE WEAK) INTERACTIONS</p> <table style="width: 100%; border: none;"> <tr> <td style="vertical-align: top;"> <p><i>Are independent of:</i></p> <p>Reflection of space Reflection of charge</p> </td> <td style="vertical-align: top;"> <p><i>Leading to conservation of:</i></p> <p>Parity Charge parity: T_3 and S</p> </td> </tr> </table> <hr/> <p>THE STRONG (BUT NOT THE ELECTROMAGNETIC OR WEAK) INTERACTION</p> <table style="width: 100%; border: none;"> <tr> <td style="vertical-align: top;"> <p><i>Is independent of:</i></p> <p>Charge</p> </td> <td style="vertical-align: top;"> <p><i>Leading to conservation of:</i></p> <p>Isotopic spin, T</p> </td> </tr> </table>	<p><i>Are independent of:</i></p> <p>Reflection of space Reflection of charge</p>	<p><i>Leading to conservation of:</i></p> <p>Parity Charge parity: T_3 and S</p>	<p><i>Is independent of:</i></p> <p>Charge</p>	<p><i>Leading to conservation of:</i></p> <p>Isotopic spin, T</p>
<p><i>Is independent of:</i></p> <p>Space translation Time translation Space rotation Zero of electric potential Inverse of space and charge together Reversal of time ?</p>	<p><i>Leading to conservation of:</i></p> <p>Momentum Energy-Mass Angular momentum Charge Product of space parity and charge reflection Time parity Baryons and leptons</p>						
<p><i>Are independent of:</i></p> <p>Reflection of space Reflection of charge</p>	<p><i>Leading to conservation of:</i></p> <p>Parity Charge parity: T_3 and S</p>						
<p><i>Is independent of:</i></p> <p>Charge</p>	<p><i>Leading to conservation of:</i></p> <p>Isotopic spin, T</p>						

THE PARAMETERS

<p>SPIN S</p>	<p>In a magnetic field, a particle with spin s can exist in $(2s + 1)$ energy states.</p>
<p>ISOTOPIC SPIN T</p>	<p>Interaction with the electromagnetic field separates particles with isotopic spin T into $(2T + 1)$ charged states.</p>
<p>PARITY EVEN OR ODD</p>	<p>The function describing a particle system remains unchanged, except for a possible change of sign, if the sign of all the spatial coordinates is changed. (space reflection). The function has odd parity if it changes sign: even if it does not.</p>
<p>STRANGENESS S</p>	<p>The charge centers of the isotopic spin multiplets within the same class are not the same. The "strangeness" number signifies the amount of this displacement. The charge centers for the two classes are chosen to be those for pions and nucleons.</p>
<p>BARYON AND LEPTON NUMBER b l</p>	<p>The baryons have $b = + 1$ for particles and $b = - 1$ for antiparticles. The leptons have $l = + 1$ for particles and $l = - 1$ for antiparticles. For baryons and mesons electric charge $Q = 0$ electron charge</p> $Q = e \left[T_3 + \frac{b}{2} + \frac{S}{2} \right]$

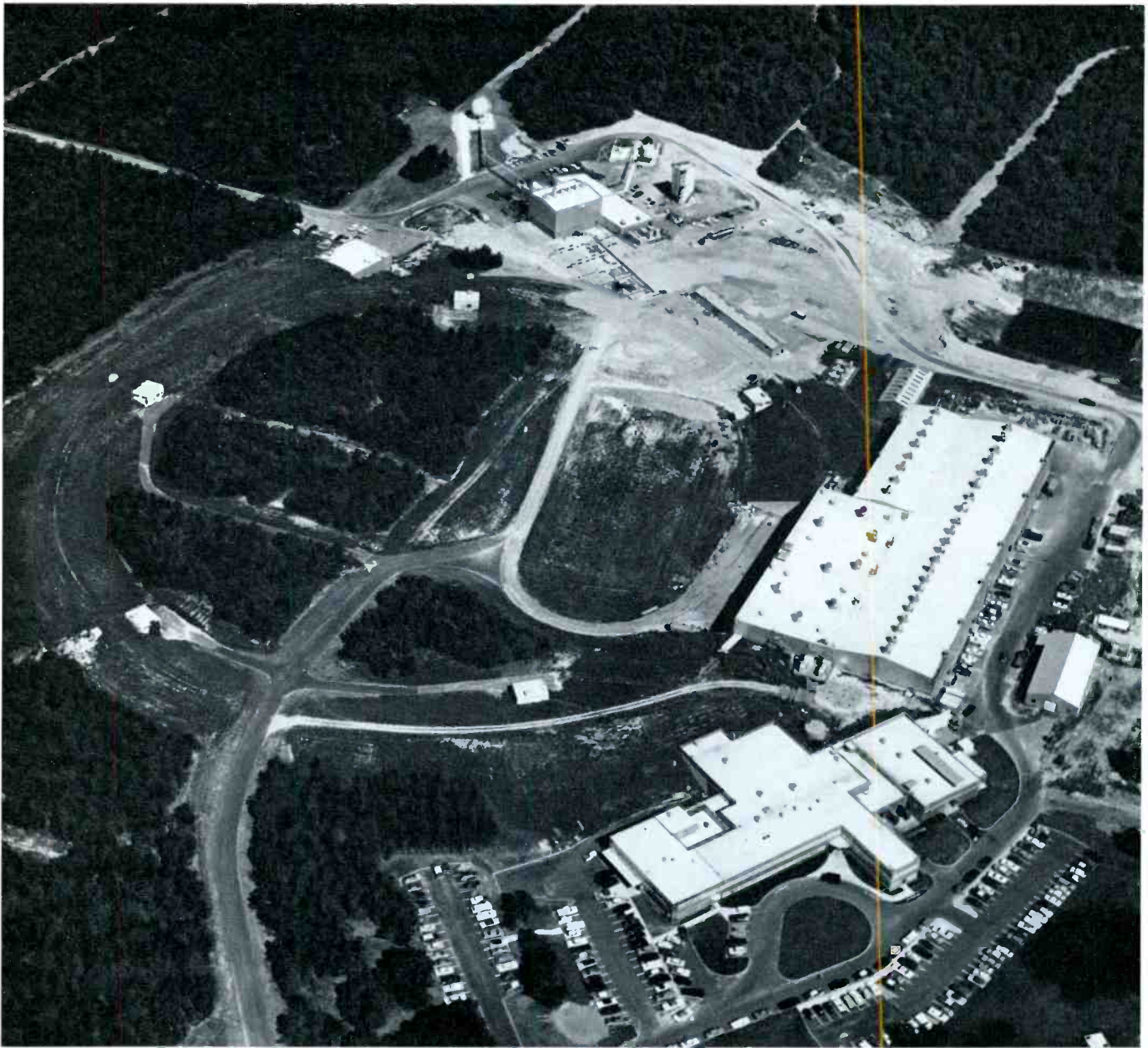


Figure 1 — Aerial view of the Brookhaven AGS.

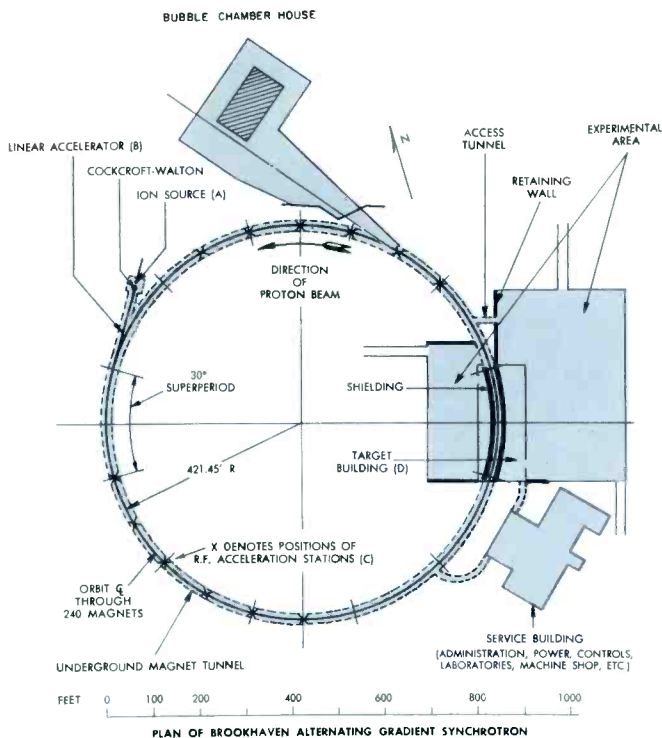
Description of the AGS

The discovery of the strong-focusing principle made feasible the design and construction of accelerators in the energy range of tens of billions of electron volts. Two such machines now exist in the 28 to 33 billion electron volt range. The first is at the European Organization for Nuclear Research (CERN) in Geneva, Switzerland. The second, and somewhat larger, is in operation at Brookhaven National Laboratory, having produced an initial beam of accelerated protons July 29, 1960.

Perhaps the most direct way to describe such a machine is to follow a beam of protons from the point of origin until

they attain the full design energy of the machine. An aerial view and a schematic representation of the Brookhaven AGS are given in Figures 1 and 2, respectively. At point (A), Figure 2, protons are obtained by ionizing hydrogen gas in a cold discharge source. Acceleration commences with the raising of these charged particles to 750,000 electron volts (ev) by means of a Cockcroft-Walton generator, illustrated in Figure 3. It is simply a high-potential transformer-rectifier-capacitor-multiplier arrangement with an RC filter for reducing ac ripple.

In the second step, protons from the Cockcroft-Walton generator are accelerated to 50 million electron volts (Mev)



- AGS peak energy
- Accelerated particles
- Circumference of synchrotron
- Accelerating cycle
- Ion source
- Preaccelerator
- Injector
- Main bending and focusing magnets
- Magnet power supply
- Vacuum chamber
- Vacuum pumps
- Accelerating stations
- Target building
- Out-door experimental area
- Enclosed experimental area
- Shielding in target building
- Power and control cable

Figure 2 — Plan of Brookhaven Alternating Gradient Synchrotron.

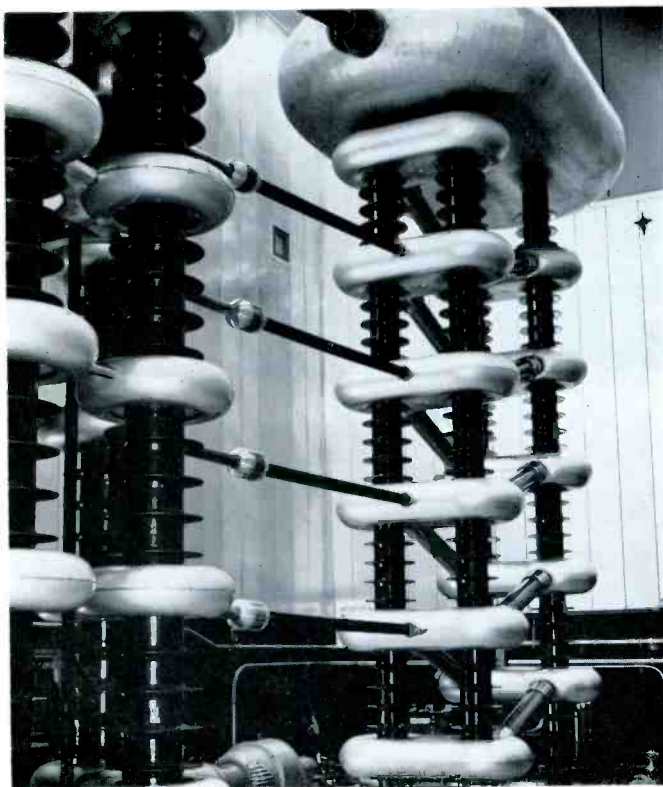


Figure 3 — Cockcroft-Walton generator.

by projecting them down the central axis of the 110-foot linear accelerator tank (Linac), point (B). The interior of this tank, viewed from the low-energy end, is shown in Figure 4. It is approximately three feet in diameter, with 124 high voltage drift tube electrodes axially spaced, shaped, and excited at resonance with several megawatts of long-pulse 200-megacycle rf power to impart the needed beam energy.

From the Linac, the 50-Mev protons are launched into the half-mile closed vacuum orbit of the synchrotron. Spaced around this orbit in twelve equal superperiods are two hundred and forty AG (i.e., alternating gradient) electromagnets weighing 4400 tons, for bending the accelerating beam while focusing it into pencil-thin bundles of particles (hence, "strong-focusing"). Simultaneously, ferrite-loaded dc biased tuned cavities do the actual beam accelerating at the twelve stations (C), Figure 2, with high-level rf power controlled by proton beam commands. Each station gives the beam an 8000-volt "kick" every revolution, making the energy gain for each orbital turn 96,000 electron volts.

In a 1.1-second magnet excitation-beam acceleration cycle, the particles make more than 340,000 revolutions (over 170,000 miles) synchronized with the rising magnet field and with the phase of the rf voltage waveform. Internal targets may be pushed into the beam's path, or the beam may be deflected out to the target building and experimental areas (D), or both. Figure 5 is a photograph of a typical nuclear event occurring in an external hydrogen bubble

33 Bev
 Protons
 About 1/2 mile in a tunnel 18-foot-square cross-section
 20 pulses per minute
 Cold discharge in hydrogen atmosphere
 750-Kev Cockcroft-Walton generator
 110-foot-long 50-Mev linear accelerator
 240 units each weighing about 20 tons, maximum corrected field 13,000 gauss
 12 phase 36,000 kva alternator dc to magnets 6000 volts, and current rising from 0 to 6500 amps, in 1.1 seconds
 0.078" thick, oval shape 3 1/4" vertical axis, 7" horizontal axis
 Dry type evaporated titanium gettering. Linac tanks 1X10⁻⁶ mm of hg. synchrotron chamber 3X10⁻⁶ mm of hg.
 12 power amplifiers rated at 20 kilowatts, output rf power frequency range 1.4 to 4.5 megacycles
 100 ft. wide x 250 ft. long
 30,000 sq. ft.
 60,000 sq. ft.
 14,000 tons of concrete
 Over 2,000,000 linear ft.

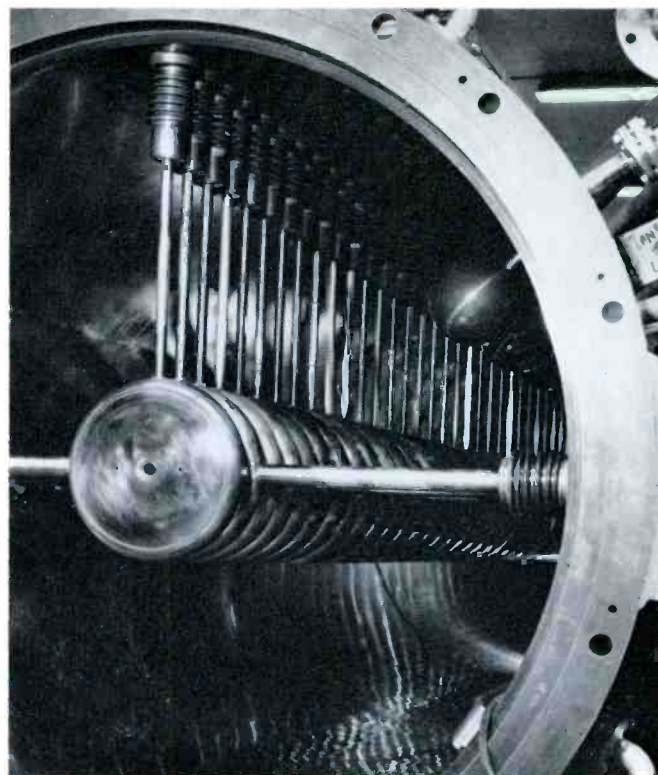


Figure 4 — Linac tank, viewed from low-energy end.

chamber.

During the following two seconds the stored magnetic energy (14 million joules) is returned to the 47-ton flywheel of a 5500-horsepower motor generator for re-use in the next magnet excitation cycle.

AGS Beam Dynamics²

In conventional circular magnetic accelerators, the particles are confined to their equilibrium orbits by magnetic focusing forces obtained by shaping the radial magnetic field so that

$$0 < n < 1, \quad (1)$$

in which n , the field gradient index, is defined by

$$n = - \frac{r}{B} \frac{\partial B}{\partial r}, \quad (2)$$

where B is the induction and r is the orbit radius. Increasing n strengthens vertical focusing forces at the expense of the radial ones; decreasing n has the opposite effect. The narrow range of n limits the strength of both focusing forces.

Except for necessary straight sections (i.e., field-free sections), n has always been kept constant with azimuth and

²J. P. Blewett, "The Proton Synchrotron," Reports on Progress in Physics, Volume XIX (1956) pp. 37-79.

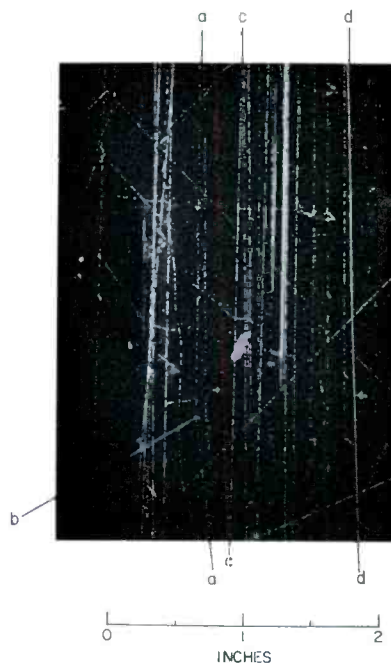


*Figure 5 — Typical nuclear event in hydrogen bubble chamber.

*Photograph showing 630 Mev/c π^+ and protons. The track aa is a π^+ that is scattered with recoil proton b. Track cc shows a beam proton, while dd is a dense background track. About half the length of the chamber is shown. The direction of the beam is from top to bottom of the picture.

relatively large magnets have had to be employed:

Machine	Location	Energy	Magnet Weight
Cosmotron	Brookhaven	3 Bev	2,200 tons
Bevatron	Berkeley	6 Bev	10,000 tons
Synchrophasotron	Dubna	10 Bev	36,000 tons

A conventional (i.e., "weak focusing") 33-Bev proton synchrotron would require more than 200,000 tons of magnet steel.

In the AGS, successive application of very strong magnetic focusing and defocusing forces of equal magnitude results in strong net focusing, reducing the orbit aperture requirement to $2\frac{3}{4}$ " height by 6" width compared with the Cosmotron's 7" by 36". A slender magnet array is achieved weighing only 4400 tons. This great reduction is explained from the Hill's equations for "betatron" oscillations in circular machines:

$$\frac{d^2r}{dt^2} + (1 - n)\omega_0^2 r = 0, \quad f_r = (1 - n)^{1/2} \frac{\omega_0}{2\pi}; \quad (3)$$

$$\frac{d^2z}{dt^2} + n\omega_0^2 z = 0, \quad f_z = (n)^{1/2} \frac{\omega_0}{2\pi}. \quad (4)$$

ω_0 is the protons' revolution frequency, and as long as $0 < n < 1$, f_r and f_z describe particle-orbit, or betatron, oscillations of the order of half the revolution frequency. In the AGS, however, $n \approx \pm 365$, and the betatron oscillation frequency becomes

$$v = \frac{N\mu}{2\pi} = 8.75 \text{ oscillations per revolution.} \quad (5)$$

N is the total number of periods of the alternating gradient system of the magnet ring, sixty in all, and μ represents the oscillatory phase shift through one such pair of focusing-defocusing elements, being defined for stability of oscillation by

$$-1 < \cos \mu < 1. \quad (6)$$

Since excursions from the equilibrium orbit for a given initial error in particle direction will be proportional to betatron wavelength (i.e., inversely proportional to betatron oscillation frequency), the effective restoring forces in the AGS are an order of magnitude greater than in a weak-focusing machine.

This economy in size and weight is achieved only at the cost of highly precise shaping and positioning of the individual magnets. The net focusing effect, while strong, is not nearly as strong as the individual forces which follow one another in opposing senses. Therefore, small misalignments of individual magnets cause large orbit deviations, particularly for integral numbers of betatron oscillations per revolution. Sensitivity to such misalignments is reduced, however, by decreasing n and the number of betatron wavelengths per revolution; accordingly, the AGS has been de-

signed finally for $v = 8.75$, with alignment of magnet units held to better than half a millimeter.

The integral (i.e., resonant) n values must be avoided. These are conveniently displayed on a stability diagram, Figure 6. Operation is possible only within a small diamond-shaped area between resonances, and further restrictions of operating area arise from subsidiary resonances.

The injected particles vary among each other not only in direction but also in energy, and therefore in momentum and speed, giving rise to radial "synchrotron" oscillations in addition to the betatron oscillations. A proton injected with a momentum error $\Delta\rho$ must travel on a different orbit having a new radius r deviating from the equilibrium radius R by an amount Δr . In a weak-focusing synchrotron these quantities are related by the expression

$$\frac{\Delta\rho}{\rho} = (1 - n) \frac{\Delta r}{R}, \quad (7)$$

defining the limits of a stable, weakly damped sinusoidal oscillation in phase of the beam with respect to the equilibrium phase of the rf accelerating voltage wave of roughly a thousand cycles per second, evidenced by a radial oscillation of several inches amplitude about this new orbit.

In the AGS, however, a proton injected with a momentum error $\Delta\rho$ travels in an alternation of sinusoidal and hyperbolic-functional deviations from a new average circular orbit differing by Δr from the equilibrium orbit in accordance with

$$\frac{v^2\Delta r}{R} = \frac{\Delta\rho}{\rho}. \quad (8)$$

These oscillations are strongly damped with increasing field, and at injection will be of the order of a centimeter in amplitude. They account for the greater width than height of the AGS orbit chamber.

When the mean proton kinetic energy in a bunch is below 7.2 Bev, protons of somewhat larger than mean energy will tend to arrive sooner at the accelerating gaps because their flight time around the ring is smaller. If the rf accelerating voltage waveform is phased so that the accelerating potential across the gap is rising at each passage of the bunch, higher energy particles, arriving early, will collect a smaller energy increment from the gap than lower energy particles arriving later. This illustrates the phase-stability principle. Our word "Synchrotron" and the Russian "Synchrophasotron" arise from this fundamental requirement for capture and acceleration of particles.

Above 7.2 Bev, the particle speeds are already over 99 percent of the velocity of light, and cannot increase much more. Protons having more than the mean energy in the bunch now tend to take longer revolution times because their equilibrium orbit radius is larger than the mean for the bunch. They arrive later at the gaps and must therefore be subjected to a falling accelerating potential in order to receive smaller energy increments than the mean particle. In the AGS, this 7.2 Bev phase transition is passed without

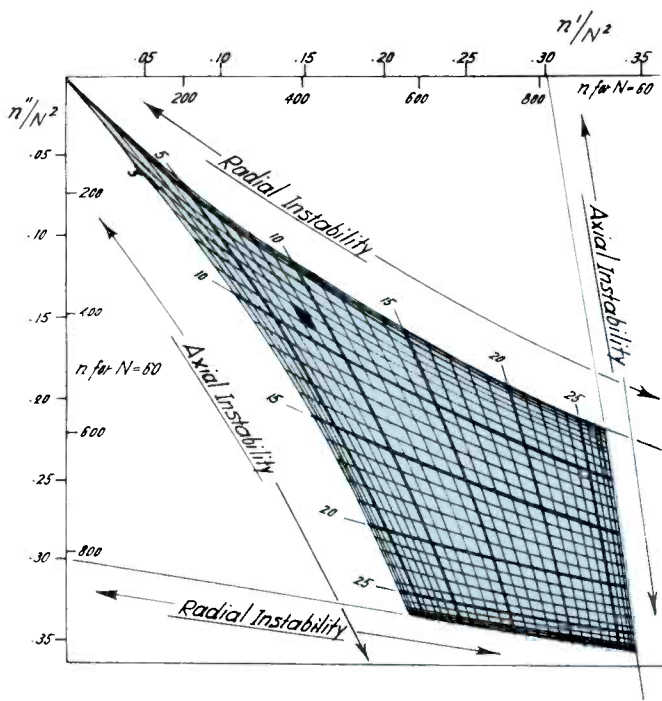


Figure 6 — Stability diagram for the AGS.

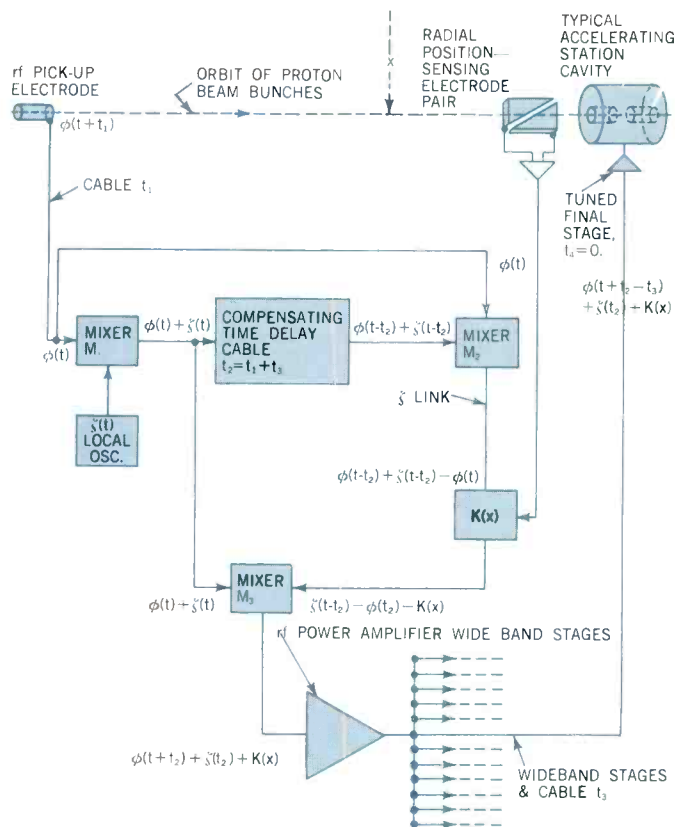


Figure 7 — Principle of phase lock rf acceleration.

generating radial excursions of the proton beam greater than those experienced earlier in the accelerating cycle, by inserting a precisely timed 120° phase step in the rf accelerating voltage waveform.

Phase Lock RF Acceleration³

It would not have been possible with conventional frequency programming to accelerate protons in the AGS and retain them within the narrow orbital restrictions of Figure 6, nor to negotiate their phase transition. Therefore a closed loop phase lock rf accelerating system has been developed whose source of commands is the protons themselves. A multiple heterodyning circuit locks the accelerating stations, rf pick-up electrodes, and circulating proton bunches into precise phase relation with each other, effectively eliminating losses of particles to the orbit chamber walls during acceleration.

With twelve identical segments or "superperiods" around the AGS orbit, it becomes convenient to employ twelve accelerating stations spaced at in-phase or out-of-phase orbital positions relative to each other. The twelfth harmonic of the proton revolution frequency is made the accelerating frequency, and a starting oscillator generating its initial value separates the injected Linac beam into twelve bunches of protons spaced equally around the ring. The starting

oscillator is then disconnected until the next injection takes place.

A continuous command rf accelerating voltage of frequency ϕ is induced upon the rf pick-up electrode, Figure 7, by the passing proton bunches⁴. It propagates in a small time interval t_1 to mixer M_1 . By this time the continuing voltage at the rf pick-up electrode will have accumulated $\phi(t_1)$ radians of phase, while M_1 will have accumulated none. After the next interval t_1 , the rf pick-up electrode will have accumulated $\phi(t + t_1)$ radians, while M_1 will have acquired $\phi(t)$. Summation of $\phi(t)$ in mixer M_1 with $\zeta(t)$ from a local constant-frequency (i.e., ζ) oscillator will have produced $\phi(t) + \zeta(t)$ radians at the input to the compensating time delay cable t_2 , and also at M_3 . Simultaneously, the output voltage from t_2 will have accumulated $\phi(t-t_2) + \zeta(t-t_2)$ radians at M_2 .

Subtractive mixing with $\phi(t)$ in M_2 provides a constant (i.e., ζ) frequency link for injecting radial phase-correcting beam commands $K(x)$ into the control loop, as well as the 120° phase-transition step and a vernier adjustment, which are not shown in Figure 7. Subtractive mixing in M_3 produces a phase accumulation $\phi(t + t_2) + \zeta(t_2) + K(x)$ radians at the input to the high power wide band rf amplifier, by the end of t .

Time interval t_3 is made the same from M_3 to each accelerating station cavity.

³M. Plotkin, "The Radio Frequency Accelerating System for the Brookhaven Alternating Gradient Synchrotron," I.R.E. 1960 International Convention Record, Part 9.

⁴H. S. Snyder, Private communication.

celerating station by cutting all the high power rf transmission cables to the same electrical length. Therefore all stations will have accumulated $\phi(t + t_2 - t_3) + \zeta(t_2) + K(x)$ radians by the end of t , and the difference in phase at that instant between the rf pick-up electrode and the accelerating stations will be

$$\phi(t + t_1) - \phi(t + t_2 - t_3) - \zeta(t_2) - K(x) = \phi(t_1 - t_2 + t_3) - \zeta(t_2) - K(x) \text{ radians.} \quad (9)$$

If the length of the compensating cable is made such that $t_2 = t_1 + t_3$, then the residual phase difference, $-\zeta(t_2) - K(x)$, will remain constant throughout the interval t . This is the desired result.

So far, all time intervals have been assumed small enough to permit regarding ϕ as constant. For larger time intervals, ϕ and its derivatives will be assumed continuous throughout the accelerating cycle, enabling expansion of (9) by Taylor's Theorem:

$$\sum_0^t \phi(t) (\Delta t) = -\zeta(t_2) - K(x) + \frac{d\phi}{dt} (t_1 - t_2 + t_3) + \frac{d^2\phi}{dt^2} \frac{(t_1 - t_2 + t_3)^2}{2!} + \dots \quad (10)$$

For $t_2 = t_1 + t_3$, all the derivative terms vanish, and the previous conclusion is again reached, namely,

$$\sum_0^t \phi(t) (\Delta t) = -\zeta(t_2) - K(x). \quad (11)$$

In the foregoing discussion, propagation times are assumed either frequency-invariant or negligibly small. Expressed in another way, the phase-frequency response of each circuit component must be linear. Otherwise, the beam of protons will make undesirable radial phase-correcting movements.

AGS RF Power Amplifier^{5,6}

At 96,000 volts per turn, about 250 kilowatts of rf power must be dissipated in the accelerating station cavities. The rf voltage wave at each one has to be locked in phase, or out of phase as the case may be, with its neighbors; its phase-frequency relation to mixer M_3 must be made essentially linear, and it must faithfully reproduce the M_3 voltage waveform. A linear amplitude transfer is requisite, while injected phase noise, ripple, harmonics, and parasitics must be suppressed. These are performance requirements for the AGS rf power amplifier.

Physically, the amplifier is a 70 db-power gain, 80 kw-output driver unit of nine ferrite-coupled balanced wide-band stages, Figure 8, energizing tuned remote final stages

⁵Brookhaven National Laboratory Patent Application S-21074, January 3, 1961, "Amplifier Apparatus for High Energy Particle Accelerator," R. H. Rhéaume, F. Janik, R. E. Zider.

⁶Brookhaven National Laboratory ADD Internal Report RHR-5, March 6, 1959, "A Parallel-Transistor Cascaded Amplifier for Controlling Very Large Currents," R. H. Rhéaume.

at the accelerating stations. The 1.4 to 4.5 mc swept rf command wave arriving from M_3 is amplified to 80 kw, then transmitted over identical coaxial cable pairs to the tuned accelerating stations, Figure 9. The wideband circuit diagram and a typical ferrite inter-stage autotransformer are shown in Figures 10 and 11. The high-level ML-6424 and ML-6696 stages are seen in Figures 12 and 13.

In these high-level stages, large zero-biased Class-A cathode-driven coaxial power triodes are coupled through centertapped step-down autotransformers, Figure 11, closely wound on large Ferroxcube 4-H toroidal cores. At lower levels, grid-driven Class-A tetrodes and pentodes are employed in similar circuits. With the triodes, no broadbanding resistors are needed because their cathode drive input impedance is self loading, the power reappearing usefully on the output side. Neutralization is unnecessary because of the excellent input-output isolation at each stage. A common 4.4 kv 220 adc plate power supply serves both the high-level wideband stages and the tuned remote final stages. The voltage transfer function for the tetrode stage network is ⁷ The corresponding Class A tetrode wideband transformer stage network is shown in Figure 14. In equation (12) it is assumed that the tetrode dynamic plate resistance is large enough to have negligible effect upon the voltage transfer function.

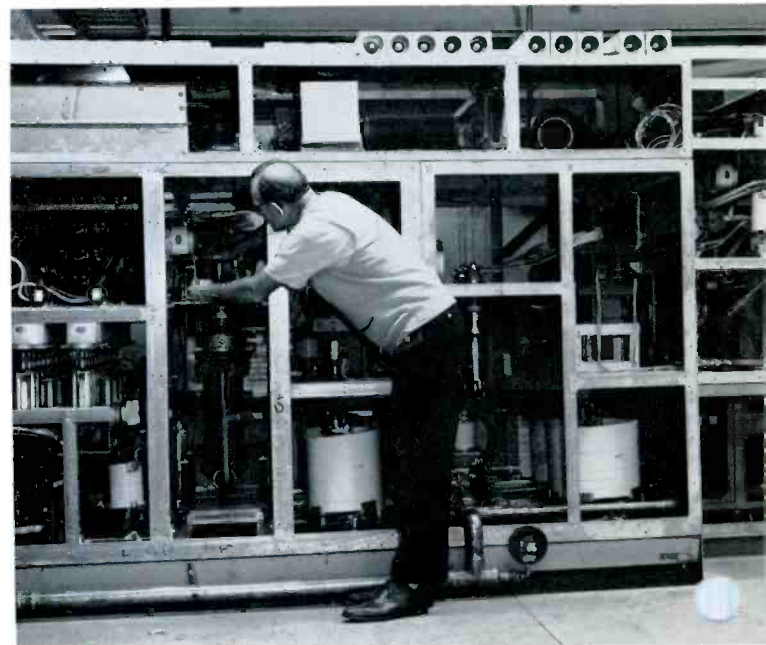
Equation (12) top next page.⁸

Figure 15 is the Class-A triode wide band transformer stage

⁷Appendix.

⁸Equations (12) and (13) are in form $X = \frac{U}{(V)(W)(Y)(Z)}$

Figure 8 — Rf high power wide-band driver amplifier stages.



$$\frac{e_0 N}{c_g} = \frac{\left(g_m N\right)\left(\frac{C_2}{C_1 C_2 + C_1 C_3 + C_2 C_3}\right)(s)\left(s + \frac{j}{L_2 C_2}\right)\left(s - \frac{j}{L_2 C_2}\right)}{\left[s + \frac{1}{2R(C_1 + C_3)} + \frac{j}{\sqrt{L_1(C_1 + C_3)}}\right]\left[s + \frac{1}{2R(C_1 + C_3)} - \frac{j}{\sqrt{L_1(C_1 + C_3)}}\right]} \left[s + \frac{1}{2R\left(\frac{C_1 + C_2}{C_1 C_2 + C_1 C_3 + C_2 C_3} - \frac{1}{C_1 + C_3}\right)} + \frac{j}{\sqrt{L_2\left(\frac{C_1 C_2 + C_1 C_3 + C_2 C_3}{C_1 + C_3}\right)}} \right] \left[s + \frac{1}{2R\left(\frac{C_1 + C_2}{C_1 C_2 + C_1 C_3 + C_2 C_3} - \frac{1}{C_1 + C_3}\right)} - \frac{j}{\sqrt{L_2\left(\frac{C_1 C_2 + C_1 C_3 + C_2 C_3}{C_1 + C_3}\right)}} \right] \quad (12)$$

$$\frac{e_0 N}{e_g} = \frac{\left(\frac{\mu + 1}{R}\right)(N)\left(\frac{C_2}{C_1 C_2 + C_1 C_3 + C_2 C_3}\right)(s)\left(s + \frac{j}{\sqrt{L_2 C_2}}\right)\left(s - \frac{j}{\sqrt{L_2 C_2}}\right)}{\left[s + \frac{1}{R(C_1 + C_3)} + \frac{j}{\sqrt{L_1(C_1 + C_3)}}\right]\left[s + \frac{1}{R(C_1 + C_3)} - \frac{j}{\sqrt{L_1(C_1 + C_3)}}\right]} \left[s + \frac{1}{R\left(\frac{C_2 + C_3}{C_1 C_2 + C_1 C_3 + C_2 C_3} - \frac{1}{C_1 + C_3}\right)} + \frac{j}{\sqrt{L_2\left(\frac{C_1 C_2 + C_1 C_3 + C_2 C_3}{C_1 + C_3}\right)}} \right] \left[s + \frac{1}{R\left(\frac{C_2 + C_3}{C_1 C_2 + C_1 C_3 + C_2 C_3} - \frac{1}{C_1 + C_3}\right)} - \frac{j}{\sqrt{L_2\left(\frac{C_1 C_2 + C_1 C_3 + C_2 C_3}{C_1 + C_3}\right)}} \right] \quad (13)$$

network. The voltage transfer function for this triode stage network is

Equation (13) above.⁸

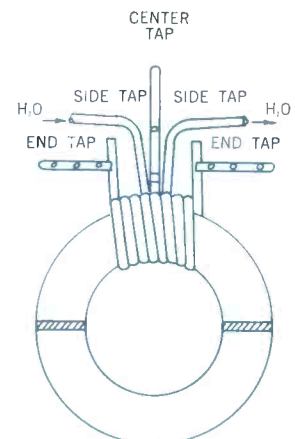
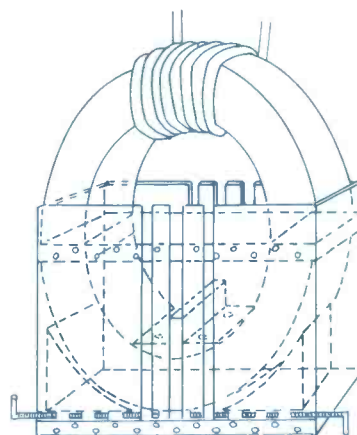
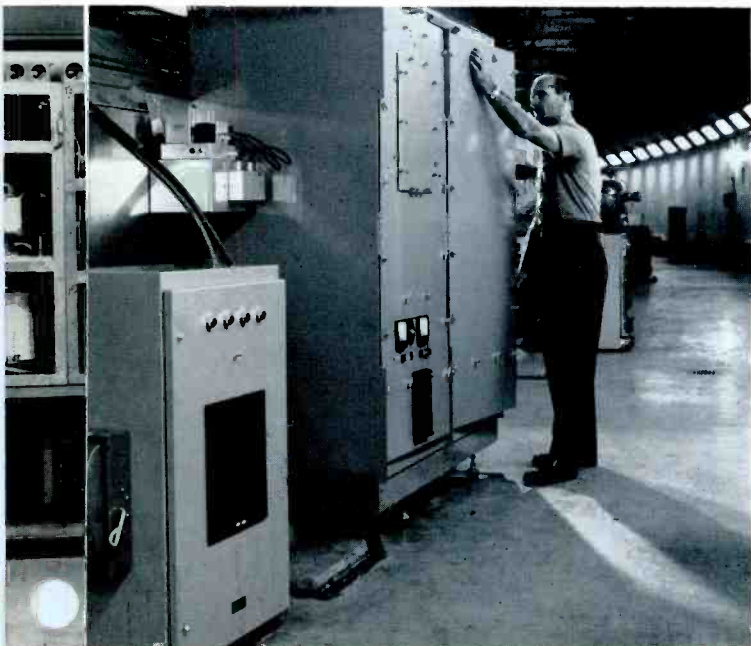
where $r_p = R$. In equations (12) and (13) it is also assumed that series leakage inductance L_2 is much smaller

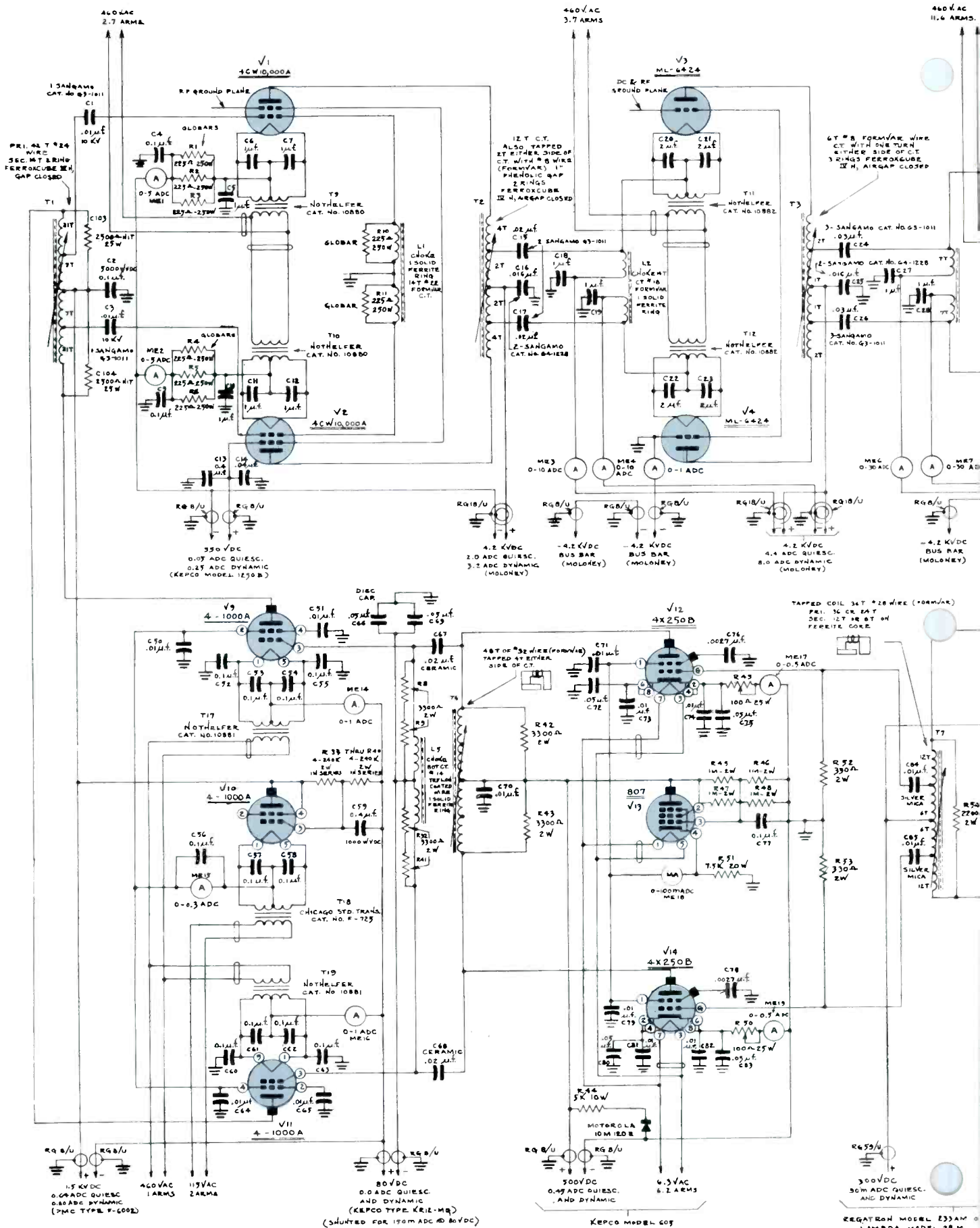
than primary inductance L_1 , that copper and core losses are negligible, and that distributive effects may be disregarded. C_1 and C_3 include terminating capacitances, and C_2 is the parasitic capacitance associated with the series leakage inductance.

Amplitude-frequency and phase-frequency responses may

Figure 9 — Typical tuned accelerating station.

Note: Figure 10 — FOLLOWING TWO PAGES.
Figure 11 — Typical ferrite interstage autotransformer.





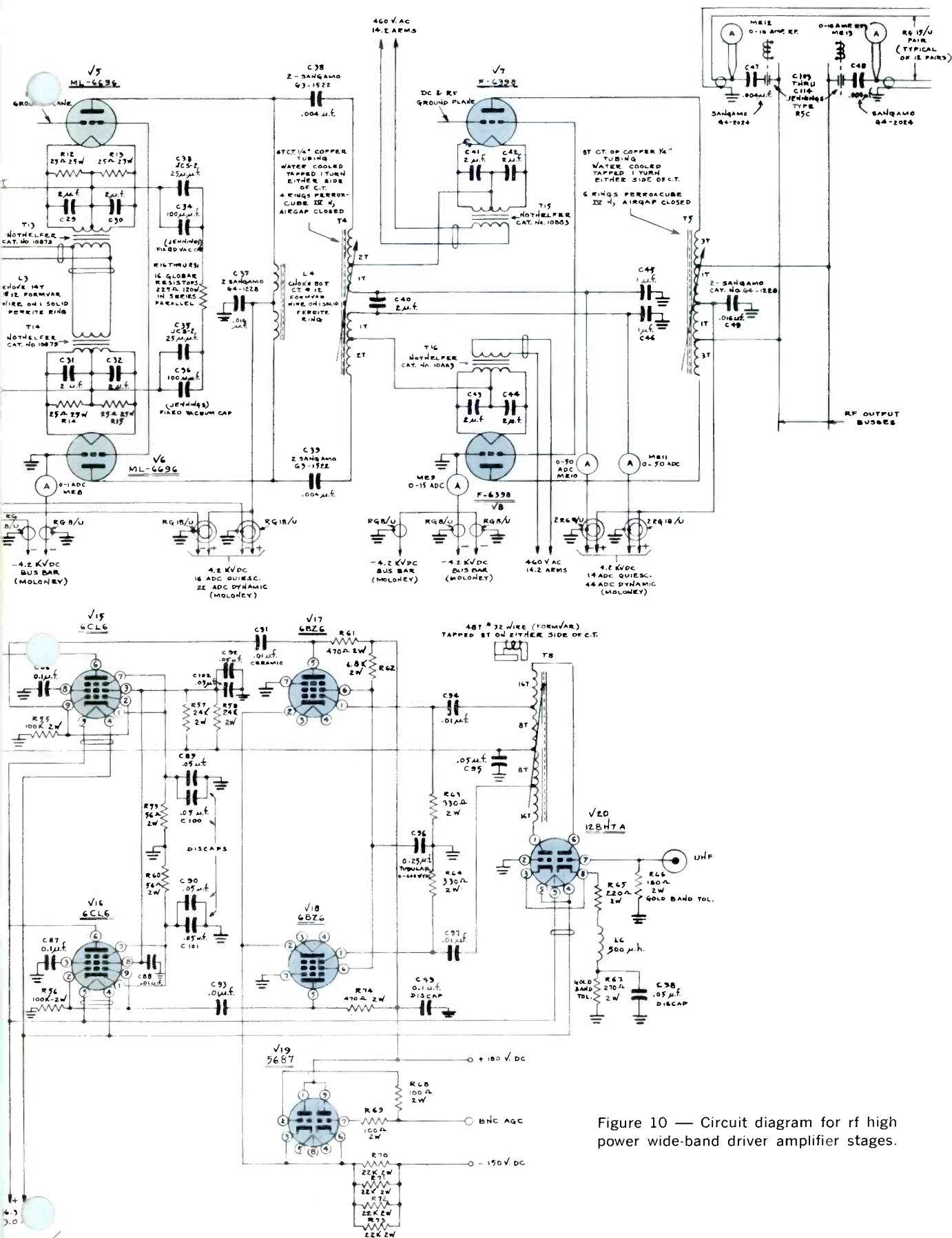


Figure 10 — Circuit diagram for rf high power wide-band driver amplifier stages.

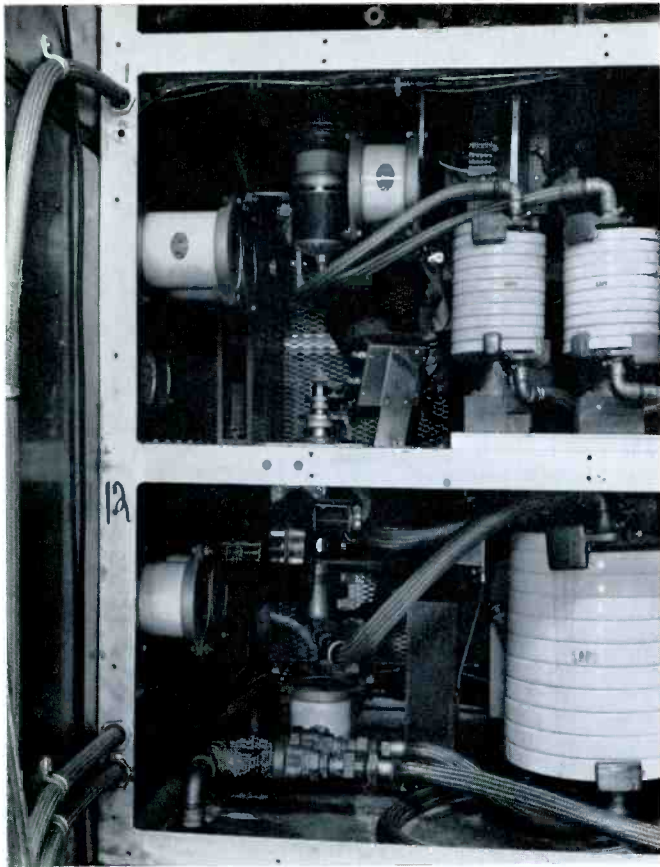


Figure 12 — ML-6424 power triode stage.

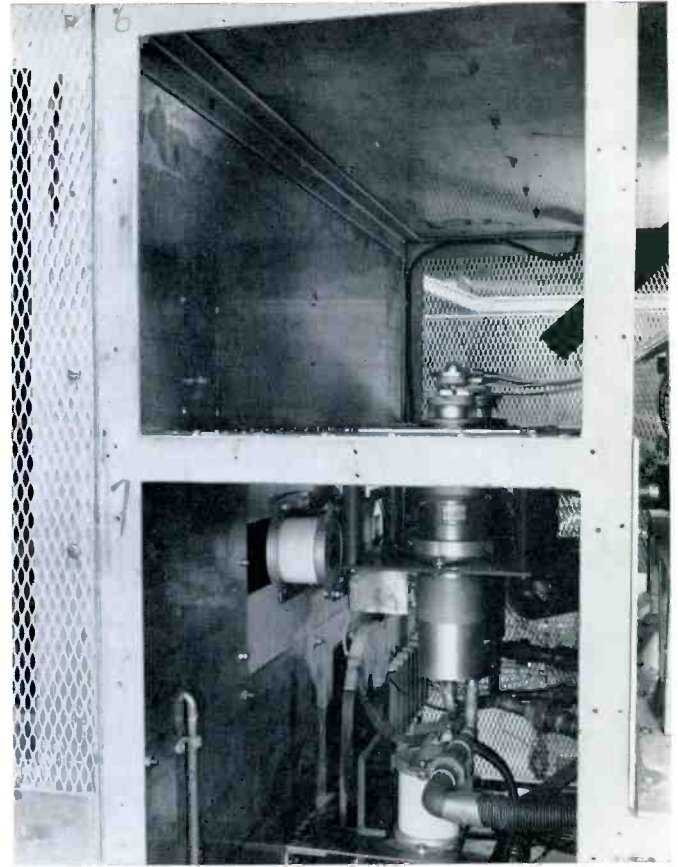


Figure 13 — ML-6696 power triode stage.

be determined by substituting real frequency points for s in equations (12) and (13) for realizable sets of circuit parameters. Balanced stages may be analyzed with composite tube characteristics^{9,10}.

APPENDIX

Derivation of Class-A wide-band transformer networks and transfer functions.

Improved stage gains and smoothness of phase-frequency response may be achieved in wide-band amplifiers for given tube capacitances with certain multipole interstage transfer functions containing finite transfer zeros arising from parasitic capacitances shunting the series inductive elements¹¹. However, in high-power wide-band interstage networks the circuit elements must be kept as few as possible to avoid unrealistically high individual element "Q's" and critical adjustments.

⁹Herbert L. Krauss, "Class-A Push-Pull Amplifier Theory," *PIRE* v 36 n 1 January, 1948, pp. 50-52.

¹⁰MIT Staff, "Applied Electronics," John Wiley and Sons, N. Y., 1943, pp. 440-446.

¹¹B. F. Barton, "Interstage Design with Practical Constraints," *IRE National Convention Record*, 1957, Part 2, pp. 154-159.

Too many elements may cause wide variations of interstage input impedance with frequency, resulting in screen or grid overloading even when the overall stage transfer function is flat. Stability should be such as to ensure constant phase and amplitude responses without trimming during the normal life of the power tubes.

Wide band interstage transformers and autotransformers offer a convenient solution for these requirements. The high-frequency equivalent transformer circuit of Figure 16(d)¹² is a three-pole low-pass filter network. By lumping the external source and load capacitances with \bar{C}_p and \bar{C}_s , and by adding the primary shunt inductance and the load resistance at the input and output ports, respectively, the Class-A tetrode wide-band transformer stage network is obtained, Figure 14. Copper and ferrite losses and the tetrode dynamic plate resistance are omitted.

$$Y_1 = sC_1 + \frac{1}{sL_1} = \frac{s^2C_1L_1 + 1}{sL_1} \quad (14)$$

¹²T. R. O'Meara, "Analysis and Synthesis with the 'Complete' Equivalent Circuit for the Wide-Band Transformer," 1961 Electronic Components Conference Proceedings, pp. 21-1 through 21-24. See also F. E. Terman, "Radio Engineers' Handbook," McGraw-Hill, N. Y., 1943, p. 370, Figure 12(b).

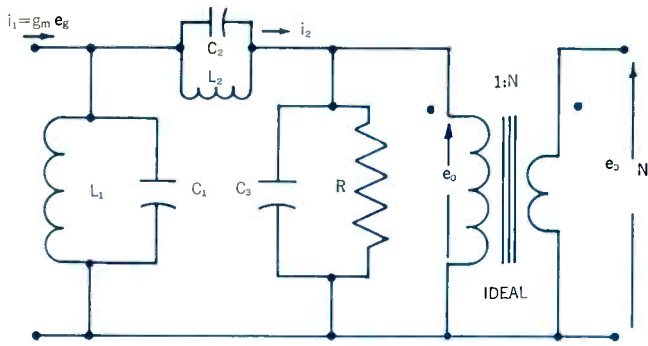


Figure 14 — Class A tetrode wide-band transformer stage network.

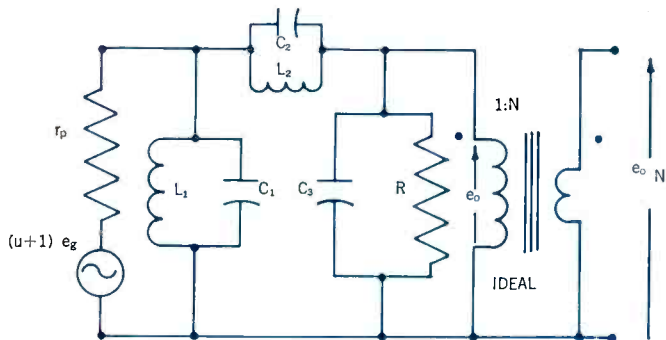


Figure 15 — Class A triode wide-band transformer stage network.

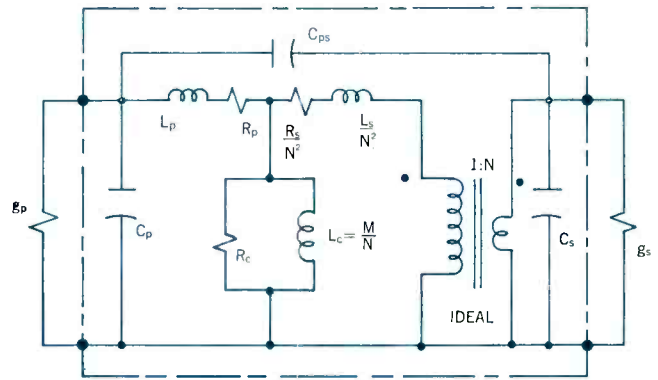


Figure 16A — "Complete" equivalent circuit for a wide-band or pulse transformer.

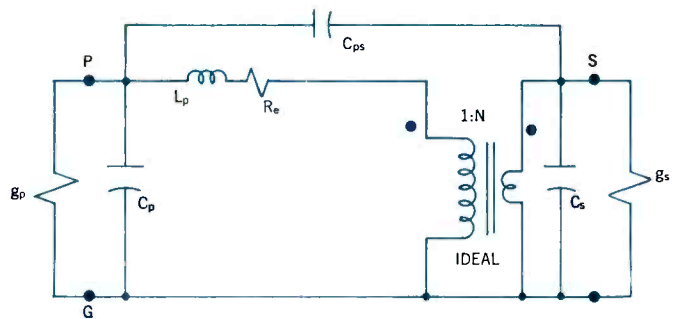


Figure 16B — Simplified low-pass filter equivalent circuit, valid for high frequencies.

$$Z_1 = \frac{sL_1}{s^2 C_1 L_1 + 1} \quad (15)$$

$$Y_2 = sC_2 + \frac{1}{sL_2} = \frac{s^2 C_2 L_2 + 1}{sL_2} \quad (16)$$

$$Z_2 = \frac{sL_2}{s^2 C_2 L_2 + 1} \quad (17)$$

$$Y_3 = sC_3 + \frac{1}{R} = \frac{sC_3 R + 1}{R} \quad (18)$$

$$Z_3 = \frac{R}{sC_3 R + 1} \quad (19)$$

$$(i_1 - i_2)Z_1 = i_2(Z_2 + Z_3) \quad (20)$$

$$i_1 = \frac{i_2(Z_2 + Z_3)}{Z_1} \quad (21)$$

$$i_2 = \frac{e_0}{Z_3} \quad (22)$$

(22) into (21):

$$\frac{e_0}{i_1} = \frac{Z_3 Z_1}{Z_2 + Z_3} \quad (23)$$

(15), (17), (19) into (23):

$$\frac{e_0}{i_1} = \frac{\left(\frac{R}{sC_3 R + 1}\right)\left(\frac{sL_1}{s^2 C_1 L_1 + 1}\right)}{\frac{sL_1}{s^2 C_1 L_1 + 1} + \frac{sL_2}{s^2 C_2 L_2 + 1} + \frac{R}{sC_3 R + 1}} \quad (24)$$

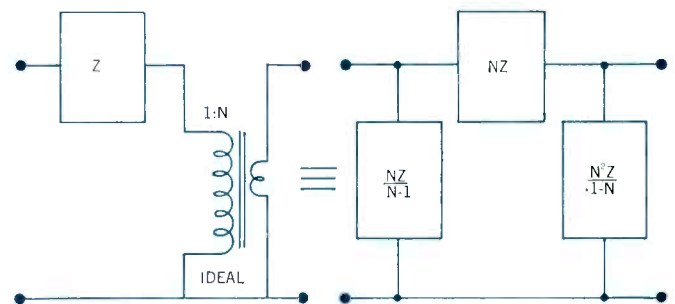


Figure 16C — Network transformation useful in deriving equivalent circuits for a transformer, valid for high frequencies.

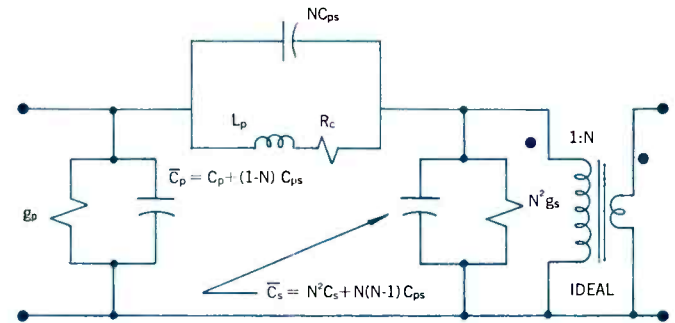


Figure 16D — Transformed equivalent circuit for a transformer, valid for high frequencies, identical to that in Figure 16B.

After expanding, regrouping, and making the assumption $L_1 \gg L_2$, (24) becomes:

$$\frac{e_0}{i_1} = \frac{\left(\frac{C_2}{C_1C_2 + C_1C_3 + C_2C_3}\right)(s)\left(s^2 + \frac{1}{C_2L_2}\right)}{\left[s^4 + \frac{s^3(C_1 + C_2)}{R(C_1C_2 + C_1C_3 + C_2C_3)} + \frac{s^2(C_1 + C_3)}{L_2(C_1C_2 + C_1C_3 + C_2C_3)} + \frac{s}{L_2R(C_1C_2 + C_1C_3 + C_2C_3)} + \frac{1}{L_1L_2(C_1C_2 + C_1C_3 + C_2C_3)}\right]} \quad (25)$$

The denominator of (25) will be factored by Lin's¹³ method. It takes the form:

$$s^4 + B_3s^3 + B_2s^2 + B_1s + B_0 = 0. \quad (26)$$

A trial divisor is formed from the last three terms of (26);

$$s^2 + \frac{B_1}{B_2}s + \frac{B_0}{B_2} \quad (27)$$

where $B_0 = \frac{1}{L_1L_2(C_1C_2 + C_1C_3 + C_2C_3)}$ (28)

$$B_1 = \frac{1}{L_2R(C_1C_2 + C_1C_3 + C_2C_3)} \quad (29)$$

$$B_2 = \frac{C_1 + C_3}{L_2(C_1C_2 + C_1C_3 + C_2C_3)} \quad (30)$$

Inserting (28), (29), (30) in (27) and simplifying, the trial divisor becomes

$$s^2 + \frac{s}{R(C_1 + C_3)} + \frac{1}{L_1(C_1 + C_3)} \quad (31)$$

Dividing (31) into the denominator of (25) and neglecting the small remainder, the resulting dividend is:

$$s^2 + \frac{s}{R} \left[\frac{C_1 + C_2}{C_1C_2 + C_1C_3 + C_2C_3} - \frac{1}{C_1 + C_3} \right] + \left[\frac{C_1 + C_3}{L_2(C_1C_2 + C_1C_3 + C_2C_3)} - \frac{1}{L_1(C_1 + C_3)} - \frac{C_1 + C_2}{(C_1C_2 + C_1C_3 + C_2C_3)(C_1 + C_3)R^2} + \frac{1}{(C_1 + C_3)^2(R^2)} \right] \quad (32)$$

For the range of component magnitudes of practical interest, (32) may be further simplified:

$$s^2 + \frac{s}{R} \left[\frac{C_1 + C_2}{C_1C_2 + C_1C_3 + C_2C_3} - \frac{1}{C_1 + C_3} \right] + \left[\frac{C_1 + C_3}{L_2(C_1C_2 + C_1C_3 + C_2C_3)} \right] \quad (33)$$

Expressions (31) and (33) may now be factored by the quadratic formula, taking advantage in each case of the relatively small magnitude of the coefficient of s for simplifying the portion under the radical sign:

$$s_{p1}, s_{p1}^* = -\frac{1}{2R(C_1 + C_3)} \pm j\sqrt{\frac{1}{L_1(C_1 + C_3)}} \quad (34)$$

$$s_{p2}, s_{p2}^* = -\frac{1}{2R} \left(\frac{C_1 + C_2}{C_1C_2 + C_1C_3 + C_2C_3} - \frac{1}{C_1 + C_3} \right) \pm j\sqrt{\frac{1}{L_2} \frac{(C_1C_2 + C_1C_3 + C_2C_3)}{(C_1 + C_3)}} \quad (35)$$

¹³Shih-Nge Lin, "Methods of Successive Approximations of Evaluating the Real and Complex Roots of Cubic and Higher Order Equations," *J. Math. Phys.*, Vol. 20, No. 3, August 1941. V. Del Toro and S. R. Parker, "Principles of Control Systems Engineering," McGraw-Hill, N. Y., 1960, pp. 644-647.

When equations (34) and (35) are substituted in the denominator of (25), and $g_m e_g$ for the driving tetrode is substituted for i_1 in (25), and both sides of (25) are then multiplied by $g_m N$, equation (12) is obtained.

Figure 15 and equation (13) for the Class-A grounded grid triode are derived from the substitution of $(\mu + 1) e_g$ in series with the triode dynamic plate resistance r_p at the input port of Figure 14 in place of $i_1 = g_m e_g$, then assuming that $r_p = R$, the transformed load resistance. The derivation of equation (14) then proceeds in a fashion similar to that for equation (13).

The additional input loading of Class-A₂ grounded grid triode operation has no effect upon equation (13), but does slightly lower the magnitude of the load resistance presented to the previous stage.

Tube Life of ML 6421F vs. ML 5667 at Station WWV

Radio Station WWV, of the National Bureau of Standards, broadcasts continuous standard frequency and time signals on six different frequencies. WWV has been using Machlett ML-6421F triodes as replacements for ML-5667 tubes originally installed in all final audio and radio frequency stages of four high power transmitters, operating at 5, 10, and 15 megacycles, respectively. Tube life data of the newer ML-6421F, which has a thoriated tungsten filament, and ML-5667, which has a pure tungsten filament, has been carefully recorded. The following is a tabulation of this data as of July 17, 1963.



ML-5667 (Pure tungsten filament)

In RF service: 14 tubes; avg. life 16,128 hours per tube
 In Mod. service: 9 tubes; avg. life 23,669 hours per tube
 In combined service: 23 tubes; avg. life 19,898 hours per tube

ML-6421F (Thoriated tungsten filament)

In RF service: 8 tubes; avg. life 47,134 hours per tube
 In Mod. service: 4 tubes; avg. life 55,460 hours per tube
 In combined service: 12 tubes; avg. life 49,826 hours per tube

To date, in RF service, thoriated tungsten filament tubes have given almost 3 times the life of pure tungsten tubes; in Modulator service thoriated tungsten tubes have given over twice the life of pure tungsten filament tubes; in combined service the thoriated tungsten filament tubes have given over $2\frac{1}{2}$ times the life of pure tungsten tubes. All 12 original thoriated tungsten tubes are still in operation.

TRANSMITTER FREQUENCY	TUBE TYPE	SERIAL NUMBER	TUBE POSITION	HOURS LIFE AS OF 7-17-63	ORIGINAL INSTALLATION DATE**
5 Mc	ML-6421F	428425	RFL	53,126	5-7-56
	ML-6421F	426798	RFR	53,126	5-7-56
	ML-6421F	425856	ML	58,435	7-13-55
	ML-6421F	425857	MR	58,435	7-13-55
10 Mc	ML-6421F	426800	RFL	50,846	4-5-56
	ML-6421F	428328	RFR	50,846	4-5-56
	ML-6421F	426791	ML	52,486	12-14-55
	ML-6421F	426801	MR	52,486	12-14-55
15 Mc	ML-6421F	428330	RFL	51,167	10-18-56
	ML-6421F	425611	RFR	51,167	10-18-56
	ML-5541	410224	ML	70,072	10-9-53
	ML-5541	410108	MR	70,072	10-9-53

LEGEND: RFL — Radio Frequency, Left ML — Modulator, Left
 RFR — Radio Frequency, Right MR — Modulator, Right

General Operating Conditions per tube:

	FILAMENT VOLTS*	PLATE VOLTS	PLATE AMPERES
Modulator — 6421	6.0 A.C.	6000 D.C.	0.1
5541	5.3 A.C.	6000 D.C.	0.1
Radio Frequency	6.0 A.C.	6000 D.C.	0.9

Modulators have static current of 0.1 Amperes. They are pulsed with a 5 cycle burst of 1000 cycles once per second, and voice and telegraphic code announcements for approximately 30 seconds out of each 5 minutes.

*Filament voltage metered, recorded a minimum of once per day; filaments operate within ± 0.1 volt.

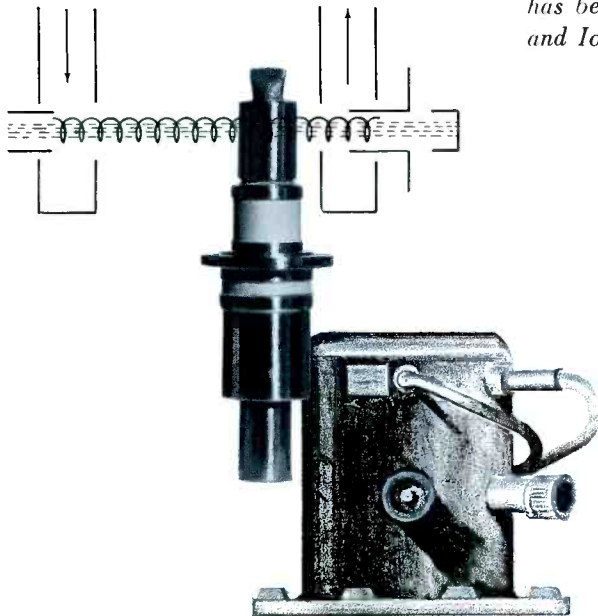
Care and attention to operation of tubes at WWV are, of course, excellent and contribute to their very substantial life figures.

**There have been no tube failures in this group of thoriated tungsten filament tubes. All tubes are still in operation.

Editor's Note:

The Committee on Thermionics and Ionics has been established by engineering groups from Raytheon Company and its affiliates to provide information of advanced technological interest to the Company. Of the two seminars held in 1963, "Vacuum Technology" and "Tubes in Space," CATHODE PRESS is pleased to print three of the papers given at the latter meeting. "The Impact of Space Environment on Electron Tube Design" by R. C. Hergenrother, Spencer Laboratory; "CW Amplitrons for Space Communications" by W. W. Teich, Spencer Laboratory; and "Negative Grid Tubes for Space Applications" by W. Brunhart, The Machlett Laboratories.

Dr. Peter F. Varadi of The Machlett Laboratories, Inc., has been the Chairman of the Committee on Thermionics and Ionics since its inception.





DR. R. C. HERGENROTHER

Dr. R. C. Hergenrother is Consulting Engineer to Spencer Laboratory on all types of present and forward looking programs. He was appointed to this position in May, 1962.

He received the degree of Bachelor of Arts from Cornell University in 1925. He went to Pennsylvania State College in 1927 as an instructor in physics and received the degree of Master of Science in Physics from that school in 1928. He continued his graduate studies at the California Institute of Technology, where he did research on X-ray crystal structure analysis, and was awarded the degree of Ph.D. cum laude in 1931.

Dr. Hergenrother joined Raytheon in 1945 as a senior engineer, and served as Manager of the Beam Tube Laboratory from 1950-62. Half a dozen patents have been issued and others are pending from his work at Raytheon. He has published articles and presented papers on camera tubes, color television tubes, storage tubes, electron optics, reflex klystrons, magnetic focus backward-wave oscillators, and electrostatic focus backward-wave oscillators.

The Impact of Space Environment on Electron Tube Design

By Dr. R. C. HERGENROTHER, Spencer Laboratory, Raytheon Company

The Evolutionary Process

Electron tubes, as well as other man-made devices, can be thought of as progressing through a process of evolution analogous to that which we see operating in nature. The environment in which the device is fabricated and used has a dominant effect on the form and capabilities of the device.

Earthbound Environment

The evolution of electron tubes started in an earthbound environment which had both advantages and problems. For example, the earth is a virtually infinite thermal sink, so there is no problem for heat dissipation. On the other hand, the atmosphere is a handicap to many fabrication processes such as metallurgy, which becomes a very "dirty" process. The problem of enclosing the electron tube in a gas-tight envelope having electrically insulated leads passing through

it and containing windows for rf radiation is sometimes formidable. The problem of exhausting, baking and sealing the envelope require a complex, costly and time consuming technique.

Airborne Environment

When electron tubes became airborne, additional requirements of increased ruggedness and decreased weight were added to those already existing and thermal dissipation became less easy.

Space Environment

The advent of spaceborne vehicles, however, introduced a new environment which differs radically from the terrestrial environment. The ultrahigh vacuum, the low temperature, the high energy particle radiation, and the limited thermal capacity of an isolated system, each raises its own problem

for the electron tube designer. How some of these problems may be met and others turned to advantage will next be considered.

Primary Requirement for Spaceborne Electronics Reliability

The electronic systems in spaceborne vehicles serve functions of communication, control, and, in some instances, propulsion. The cost of launching a vehicle is very high and once it is spaceborne, it is inaccessible for modification or repair in the usual sense. This places a high premium on reliability of the components comprising such systems.

Efficiency

Another requirement which is second only to reliability is high efficiency. Improvements in efficiency are reflected immediately in decreased power input requirement, and thus, in size and mass of power source and power conversion devices. Another benefit of increased efficiency is a reduction in the thermal dissipation problem, which will be discussed later.

Minimum Mass

Any reduction of mass which may be achieved by improved efficiency or other means exerts a great leverage in that this reduces the power required for launching and the powers required for propulsion.

Electron Tubes versus Solid State Electron Devices

It is important to raise the question regarding which, if any, functions of spaceborne electronic systems are best performed by solid state electron devices and which are best performed by electron tubes.

Solid state devices are compact and have a potential of long life capability. Their power output capability, however, is limited and their frequency-bandwidth capability is also limited. Solid state devices are affected by high energy particle radiation and must be adequately shielded if required to operate in regions of high density, high energy particles, as for example the Van Allen belt. High temperature processing, such as sterilization, can also cause deterioration of some solid state devices.

Electron tubes, on the other hand, can have a high power output capability and also have a wide frequency bandwidth capability. Tubes are virtually unaffected by high energy particle radiation and are not affected by high temperature processing, such as sterilization.

The best engineering trade-off of these characteristics appears to be achieved by using radiation-shielded, solid state electronics at low power levels if the frequency bandwidth requirements are within its capabilities. At power levels above one (1) watt, electron tubes are mandatory. A notable example is the Telstar communication satellite which uses solid state electronics throughout except for the power output tube, which is a traveling wave tube. It will

be recalled that the first Telstar had a failure of the solid state electronics because of insufficient shielding.

Properties of Space Environment

The radical properties of the space environment in which spaceborne electronic systems will be required to operate are listed below:

- Ultrahigh Vacuum
- Low Ambient Effective Temperature
- Virtually Zero Acceleration (Force)
- High Energy Particle Radiation
- Meteoroids
- Limited Thermal Capacity (of Vehicle)

Ultrahigh Vacuum Environment

The most favorable factor of space environment for electron tubes is the ultrahigh vacuum. This is spectacular by terrestrial standards, as shown in Table I.

TABLE I¹

Altitude	Pressure (Torr)	Molecules/cm ³
0	760	2.7×10^{19}
100 mi	10^{-6}	3.5×10^{10}
500 mi	10^{-10}	3.5×10^6
1000 mi	10^{-12}	3.5×10^4
Interplanetary	0.3×10^{-15}	10

At a pressure of one (1) Torr or one (1) millimeter of mercury, a cubic centimeter contains 3.5×10^{16} molecules of gas. The achievement of pressure of 10^{-9} Torr or 3.5×10^7 molecules per cubic centimeters in sealed off tubes in the earth's environment is technically difficult. This pressure is already reached at an altitude of 300 miles above the earth's surface, and at 1000 miles the gas density is of the order of 3.5×10^4 molecules per cubic centimeter and is believed to be of the order of 10 molecules per cubic centimeter in interplanetary space.

Insulation

One benefit of a total environment of high vacuum is that this serves as the best possible insulation. This means that insulation needs are reduced to only mechanical support requirements. Limitations on conductor spacings are imposed only by electromechanical forces and by cold emission which can occur at electric fields above 10^6 volts per centimeter.

Envelopes

The high vacuum existing in space suggests the possibility of constructing the tube envelope so that it can be opened when the system is in space to achieve the benefit of a continuous high speed, ultra high vacuum pumping. Such a procedure would alleviate many common electron tube problems, such as ion oscillation effects, cathode poisoning, and gettering.

A more radical approach which may be considered is the complete elimination of an envelope. This would not only increase the pumping speed but would eliminate the need for leads and rf windows which are required in an envelope. Transmission lines for rf can be reduced or even in principle eliminated if the interaction circuit and radiator could be combined. The elimination of the rf window would eliminate the problems which these windows are subject to, such as losses, mismatch, multi-factor and breakdown.

Cathodes

The use of an openable envelope would permit the use of any type of conventional cathode which could be processed in the usual way. The elimination of the envelope would introduce new problems with respect to the cathode. It would be possible to defer activation or processing of the cathode until the system is in the space environment, in which event, any type of cathode could be used. This would, however, preclude the possibility of testing the system with

the cathode in earth environment before launch. It would be possible to test the system before launch in a bell jar which could be evacuated. The system would then be removed from the bell jar and installed in the vehicle but would not be re-activated until it was in a space environment. This procedure would preclude the use of oxide coated cathodes or similar types, but would permit the use of pure tungsten or tantalum cathodes, dispenser type cathodes, tunnel cathodes and secondary emission cathodes.

Cathode Heating

In addition to the conventional ohmic heating of thermionic cathodes, two other heating methods can be considered. It would be possible, for example, in systems which did not get too far from the sun to use solar energy directly for heating the cathode. This requires focusing the solar image on the cathode and implies orientation requirements. Another interesting approach is to use "collector-cathode" heating. In this scheme, the collector from one tube is combined with the cathode of the following tube so that the energy dissipated at the collector is used to supply the cathode heating energy. Both of these methods, which are illustrated in Figure 1, have the advantage of reducing the energy input requirements.

The ideal cathode for space environment is the tunnel cathode since this does not need to be heated and can theoretically achieve a high level of efficiency.

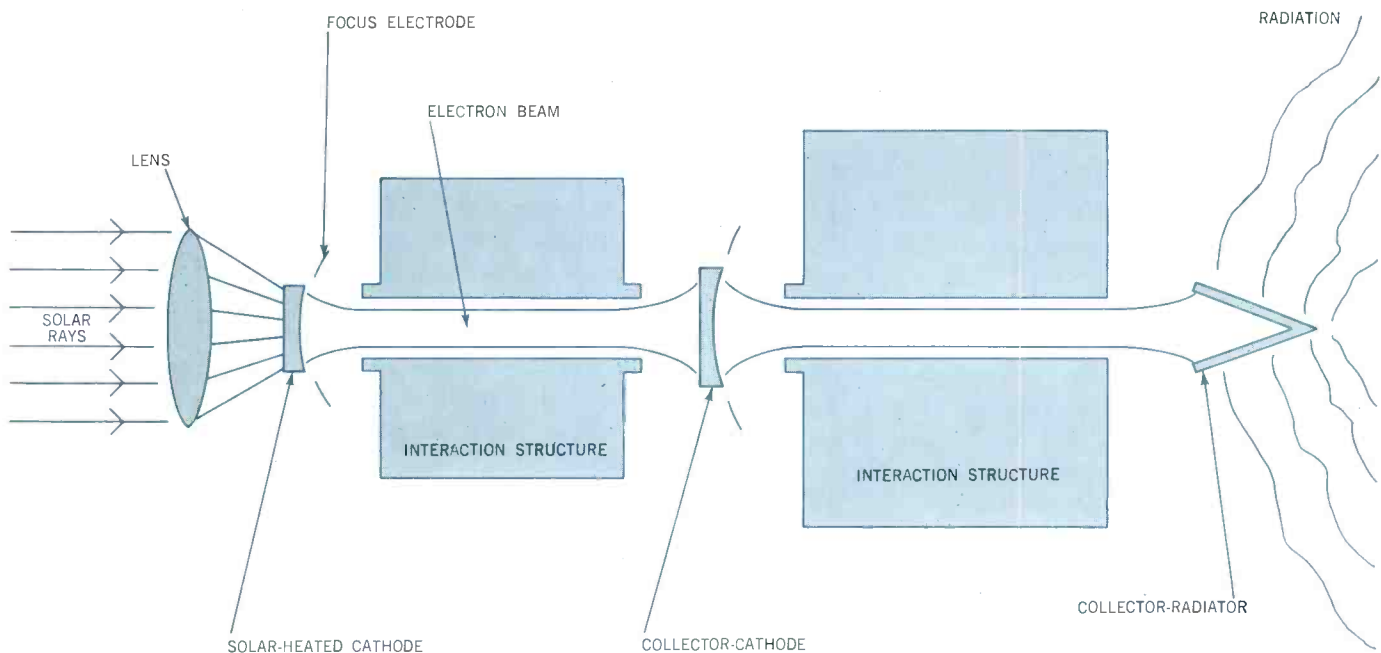


TABLE I Reference — Jastrow, R. and Kyle, H. The Earth's Atmosphere Sec. 2.1 of Handbook of Astronautical Engineering, First Ed. Heinz Hermann Kelle, ed., McGraw-Hill Book Co., Inc., 1961, pp. 2-2 - 2-13.

Figure 1 — Methods of Cathode Heating and Spent Electron Beam Power Dissipation.

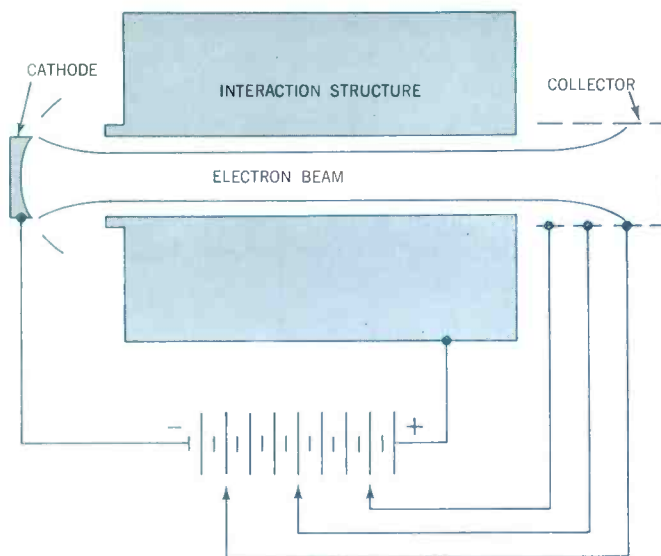


Figure 2 — Retarded Potential Collector.

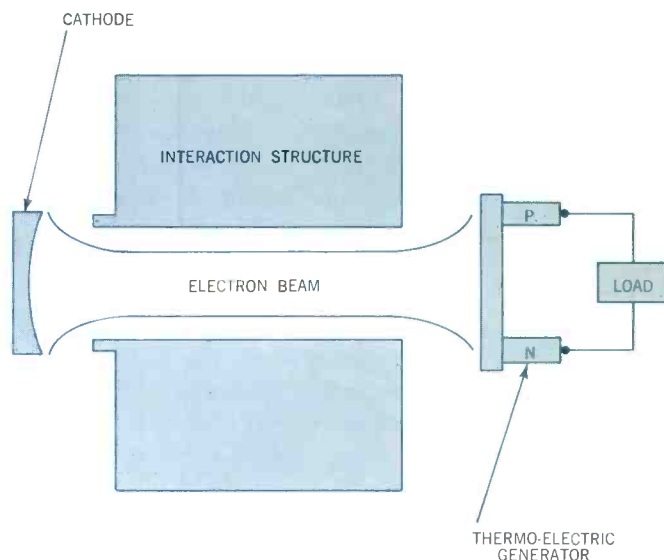


Figure 3 — Conservation of Spent Electron Beam Power.

Beam Energy Conservation

To improve the efficiency of the tube and at the same time minimize the problem of heat dissipation, maximum use should be made of the retarded voltage beam collector concept, which is shown schematically in Figure 2.

Another method of conserving energy would be to combine the target electrode with a thermoelectric generator, as indicated in Figure 3.

Beam Energy Dissipation

It might be supposed that the energy of the used electron beam could easily be disposed of by letting the electron beam be projected into free space. Such a procedure would, however, result in the build-up of a positive electric potential on the surface of the vehicle and the resultant electric field would quickly reach sufficient strength to pull the electrons back to the surface of the vehicle which would then act as a collector, as shown in Figure 4. The space charge cloud, which would build up around the vehicle, could conceivably interfere with radio communication.

The only way to get rid of residual waste thermal energy in the space vehicle is through radiation. The thermal power radiated from a surface depends on its emissivity and is proportional to the area and to the absolute temperature with exponent four. This means that doubling the temperature is equivalent to a sixteen fold increase in area. This suggests the use of a small target of tungsten, or the like, heated by the waste electron beam to a very high temperature and located in the shadow of the vehicle, as is indicated

in Figure 1.

Magnetic Field Effects

Magnetic fields in interplanetary space are extremely weak being two or three orders of magnitude lower than the earth's magnetic field. These fields then will exert no action on the electron tubes. However, any magnetic fields in the vehicle produced by focusing systems, for example, will be acted on by the earth's magnetic field when the vehicle is in the vicinity of the earth and produce a mechanical couple such as is produced on a compass needle by the earth's field. To minimize this effect, magnetic moments within the vehicle should be balanced so their vector sum is virtually zero. Periodic magnetic focus systems should have an even number of magnets, for example. Conversely, the earth's magnetic field could be used for orientation maneuvers by using solenoids through which controlled electric currents can be sent.

Meteoroids

The density of meteoroids in space is very low² and is in inverse proportion to their size. Meteoroids of 1 (one) microgram mass have an incidence of about 3 (three) particles per square meter per year, and particles of 1 (one) milligram mass have an incidence of 1 (one) particle per square meter per 300 years. Shielding would not be necessary since a 1 (one) microgram particle would have a negligible effect even if it struck the cathode and even a 1 (one) milligram particle would have only a minor effect.

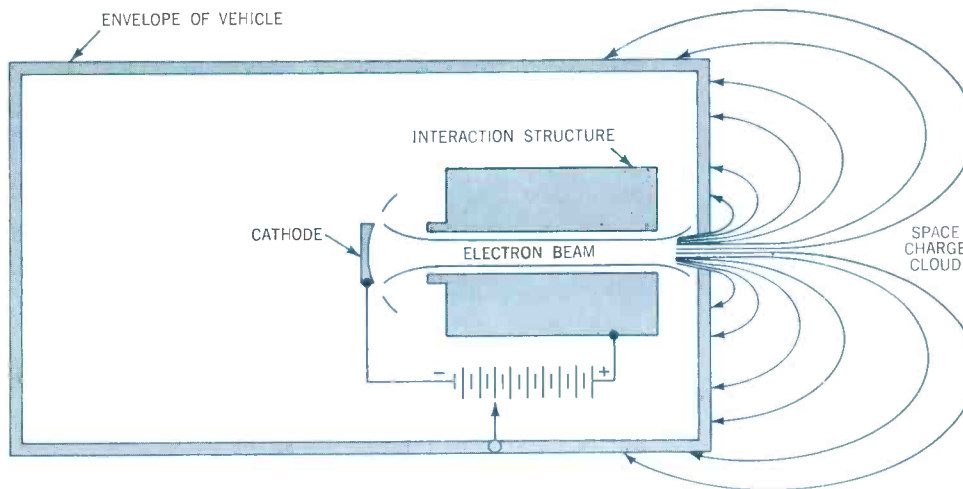


Figure 4 — Spent Electron Beam Projected into Space. (Note: If Envelope is at Cathode Potential, Electron will not penetrate Envelope Opening).

Particle Radiation

Particle radiation from cosmic rays comprises high energy protons, alpha particles and completely stripped nuclei with masses up to ten. The overall average in free space is of the order of 2.5 particles per cm^2 per sec.

Solar flares give rise to particles with energies ranging from a fraction of BEV up to 20 BEV. These occurrences are related to solar flares and the solar cycle which are not closely predictable. The most intense radiation is in the Van Allen belt comprising protons and electrons trapped in the earth's magnetic field, and in an artificial electron belt produced by a high altitude nuclear explosion of July 9, 1962 which is similarly trapped by the earth's magnetic field.

These particle radiations, particularly solar flares and trapped radiation, can have serious biological effects and are being intensively studied for this reason. The effects on solid state devices, such as transistors and solar cells, are significant and are being studied². The effects of these particles on electron tubes would be confined to their effects on insulators and these are expected to be orders of magnitude less than the effects on semiconductors. No shielding or other electron tube design considerations will be affected by these particle radiations as far as we know at present.

²Alexander, W. M., McCracken, C. W., Secretan, L. and Berg, O. E. Review of Direct Measurements of Interplanetary Dust From Satellites and Probes X-613-62-25, Goddard Space Flight Center, NASA, 1962.

Summary

In the space environment, reliability is of vital importance and is the basic factor guiding the design and construction of electronic systems. The techniques of quality control and testing must be carried to the highest level of refinement.

Second only to reliability is the requirement for high overall efficiency. This factor increases in importance with increasing power levels. Solid state electronic devices have the advantage of compactness and ruggedness. They have high reliability and long life when adequately shielded from high energy particle radiation. They are a natural choice where their frequency and bandwidth capabilities and their power handling capabilities are adequate for the required application.

At power levels above one watt, solid state microwave devices reach their present state-of-the-art limit of power output, and at higher power levels, tubes are used.

In the range of one (1) watt to 100 watts the sealed-off tube represents the simplest solution. As power is increased, it becomes more desirable to open up the envelope to outside space after the system has gone beyond the earth's atmosphere. This requires the development of simple, reliable, light-weight, one-shot vacuum tight devices. At sufficiently high power levels, the envelope-less structure with its freedom from lead through and rf windows with its simplified transmission lines becomes attractive to the designer.

³Hulten, W. C., Honaker, W. C., and Patterson, John L.: Irradiation Effects of 22 and 240 Mev Protons on Several Transistors and Solar Cells NASA TN D-718, 1961.



WESLEY W. TEICH

Mr. Wesley W. Teich is a Principal Engineer in the High Power Tube Laboratory of the Raytheon Microwave and Power Tube Division. He has been active in the development of microwave tubes since joining the company in 1945, and is currently directing activity in the development of low power Amplitrons and Stabilotrons for several communications and telemetry applications.

Mr. Teich received his B.S. degree in electrical engineering from Iowa State University, Ames, Iowa, in 1945. He has since completed graduate courses in this field at the Massachusetts Institute of Technology.

He has served as a member of the IRE standards committee on operating measurements of microwave oscillators and more recently, as a member of the Technical committee on Electron Tubes.

Design of CW Amplitrons for Space Applications

By *WESLEY W. TEICH, High Power Tube Laboratory,
Raytheon Microwave and Power Tube Division,
Burlington, Massachusetts*

The requirements for microwave transmitters to be carried into space place unusual demands on the microwave tubes to be employed. To best meet these demands, not only must careful attention be paid to the design details of the device selected, but also it is important that selection of the basic device to be employed be based on proper consideration of the needs of the application.

The basic simplicity and high efficiency of the Amplitron make the device attractive for space applications. The required rf structures lend themselves well to conduction cooling at ground potential and to low mass and high rigidity which promise high resistance to modulation or

damage from severe shock and vibration. The high efficiency, of course, is reflected in low power consumption and, consequently, in minimum size and weight of the associated power supply.

Table I presents the characteristics of four Amplitrons currently being built at Spencer Laboratory for several space applications. The anode structures of these four tubes are nearly identical, but variations in the packaging arrangement and the selected operating point adapt them to specific systems. Three of these types are shown in the photograph of Figure 1.

The Amplitron is a crossed-field device and consequently

TABLE I
SPACE AMPLITRON CHARACTERISTICS

	QKS997A	QKS1051	QKS1119	QKS1200
Anode Voltage V	1800-2000	1800	2450	1500
Anode Current mA	25	22.2	50	14
Power Output W	20	22	70	10
Frequency Mc	2200-2300	2295	2295	1700
Plate Efficiency	55%	55%	60%	55%
Heater Power (Run) W	0.4	0.4	0.3	0.4
Heater Voltage Preheat V	6.3	6.3	6.3	6.3
Drive Power mW	500	450	1760	100
Cooling	Conduction	Conduction	Conduction	Conduction
Weight	24 oz.	24 oz.	32-43 oz.	24 oz.
Size	2¾ dia. x (less connectors)	2¾ dia. x 2¾ long	2¾ dia. x 3 long	2¾ dia. x 2¾ long

requires a dc magnetic field perpendicular to the basic flow of electrons from cathode to anode. In the tubes pictured the magnetic field is generated by two cylindrical magnets of Alnico VIII material. The tube anode together with the magnets are mounted inside of a steel can which provides the return path for the magnetic circuit, the thermal path from the rf structure of the anode to the cold plate on which the tube mounts, and mechanical support for the entire tube. This shell is 2¾ inches in diameter and either 3.4 inches long on the 70-watt version, or 2¾ inches long on the lower power types. The 20-watt tubes weigh

only 24 ounces.

Because of the magnetic shell, the tubes are practically immune to changes in performance due to the presence of nearby magnetic materials. The stray field from the Amplatron is less than 200 gamma (10^{-5} gauss) at a distance of 3 feet from the tube.

Figure 2 shows the basic anode assembly of the QKS997A together with the cathode, a ceramic mounting washer and one of the pole piece assemblies necessary to complete the vacuum envelope.

One rather unique feature of the Amplatron which makes



Figure 1 — Three Raytheon CW Amplitrons developed for communications. Shown (left to right) are the QKS997A, QKS1051, and the QKS1119.

it attractive for many telemetry applications is the absence of attenuation in the rf structure. With no voltage applied, the tube behaves as a bandpass filter with an electrical length of only a few half-wavelengths. Its insertion loss in either direction is of the order of 0.5 to 1.0 db (Figure 3). Most of the common failure modes, especially of low power tubes, leave this property intact, and effective redundancy can be obtained by placing two identical tubes in cascade and switching voltages to the one selected for operation at a particular time (Figure 4).

The feed-through feature also permits multi-level operation at high efficiency. In the simplest arrangement, the driver is allowed to feed through a single Amplitron stage providing two output levels differing by about 20 db.

The absence of attenuation in the Amplitron makes it often desirable to include circulators in the system design to provide non-reciprocal attenuation. In general, the driver for the Amplitron must be protected by a circulator or isolator since reflections from the Amplitron load pass through the tube unattended (and unamplified). With a 20-db gain in the Amplitron, the load would have to be kept below 1.1/1 VSWR to prevent the driver from seeing a short circuit or worse. In addition, the Amplitron itself generates reverse directed power about 20 db below the output signal, and a circulator will prevent this from affect-

ing the driver performance.

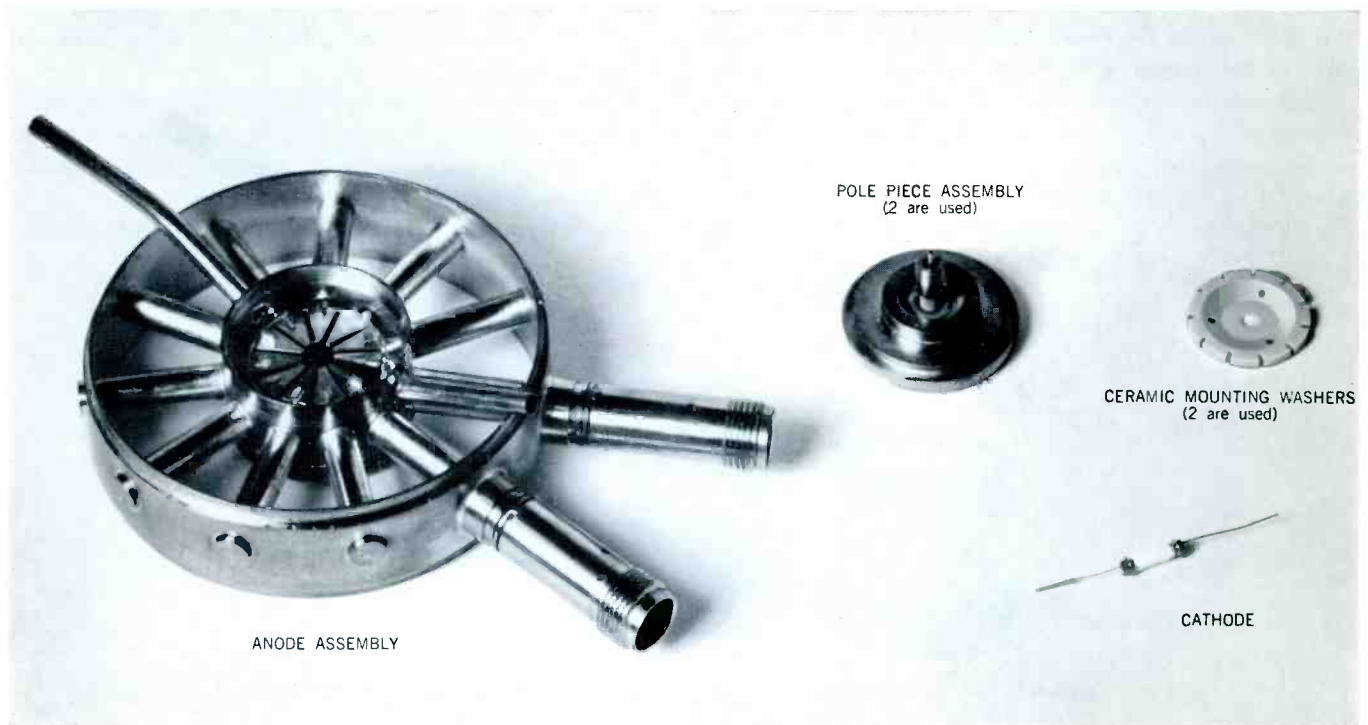
The Amplitron is a crossed-field continuous-cathode backward wave amplifier. In the QKS997, which has been developed specifically for spaceborne telemetry, an eleven-vane rf structure is employed to obtain electronic interaction with the $n = 4$ space charge mode.

The rf structure, shown in Figure 5, consists of a pair of straps forming a two-wire transmission line. This line is loaded by 11 vanes connected to alternate sides of this line. The vanes are primarily capacitive and they are shunted by coaxial cavities which are inductive (less than quarter-wavelength) at the operating frequency. Connections are made to either end of the two-wire line through coaxial line terminating in TNC female connectors. Dimensions of the coaxial lines are selected to provide appropriate impedance transformation between the anode structure and standard 50 Ω coaxial cable.

At the operating frequency, the phase shift along the two-wire line is approximately 3 half-wavelengths. The rf field distribution inside the anode hole is then 8 half-wavelengths — 11 180° phase reversals introduced by the alternate connection of the vanes minus $3 \times 180^\circ = 540^\circ$ phase delay on the straps.

Electronic interaction with the wave traveling on the anode circuit can then be obtained with a space charge

Figure 2 — Parts of Basic Anode Assembly, CW Amplitron.



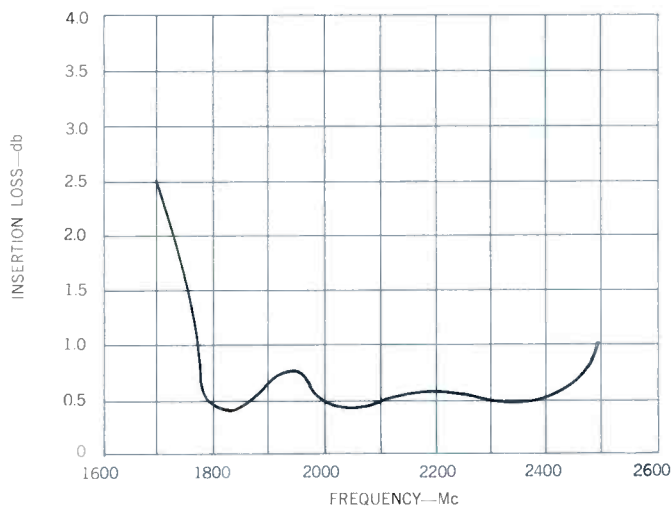


Figure 3 — QKS997A-101 Insertion loss through CW Amplitron.

distribution with four strokes, similar in many respects to the space-charge distribution in an oscillating 8-vaned magnetron. The operating parameters — magnetic field, anode voltage, efficiency — are calculated on the same basis as that of the magnetron.

In the case of the QKS997, the calculated $V_0 = 192$ volts and $B_0 = 487$ gauss at 2300 Mc. The selected operating point is $V = 1800$ volts with a magnetic field of 2200 gauss — $B/B_0 = 4.5$. For this value of B/B_0 , the theoretical efficiency is 87%. Efficiencies in excess of 60% are measured under these conditions.

The voltage-current characteristic of a CW Amplitron appears as shown in Figure 6. With rf drive present, a sharp "gauss line" or operating line appears near the voltage for optimum interaction at the frequency of the drive signal. This line is an impedance of only a few hundred ohms, compared to 500 to 100 kilohms for the static impedance of the tube. The maximum current that may be drawn on this line is a function of drive power. A plot of power output at the maximum current as a function of drive power is shown in Figure 7.

Also plotted in Figure 7 is a mathematical expression for gain in the Amplitron device derived by W. C. Brown and based on a rigid spoke theory of interaction. The power output plotted is the maximum that can be obtained by adjusting the power supply for maximum anode current at the drive level specified. The normal operating current is chosen at least 20% below this maximum level.

With the current held constant at a value less than the maximum value, varying the drive signal power has little effect on the power output. Any additional drive power above the minimum required passes through the tube and

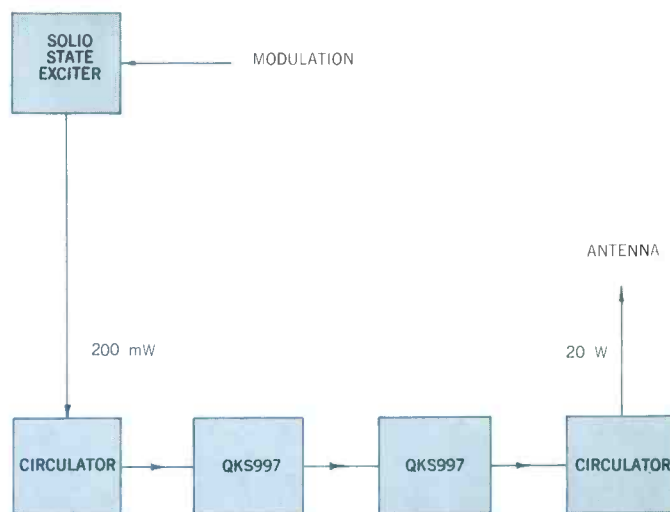


Figure 4 — Block Diagram, 20-watt Amplitron Telemetry System with redundant power stages.

adds to the output without amplification.

With no drive power applied, the Amplitron will draw reduced current and produce a noisy output signal several megacycles wide centered at a frequency which is proportional to the applied voltage.

With drive applied, the anode voltage of the Amplitron must be held within narrow limits if amplification is to be obtained. This is generally accomplished with a power sup-

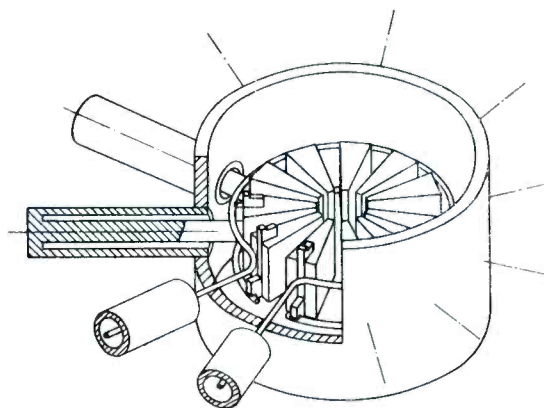


Figure 5 — Pictorial representation of the eleven-vaned rf circuit of QKS997A.

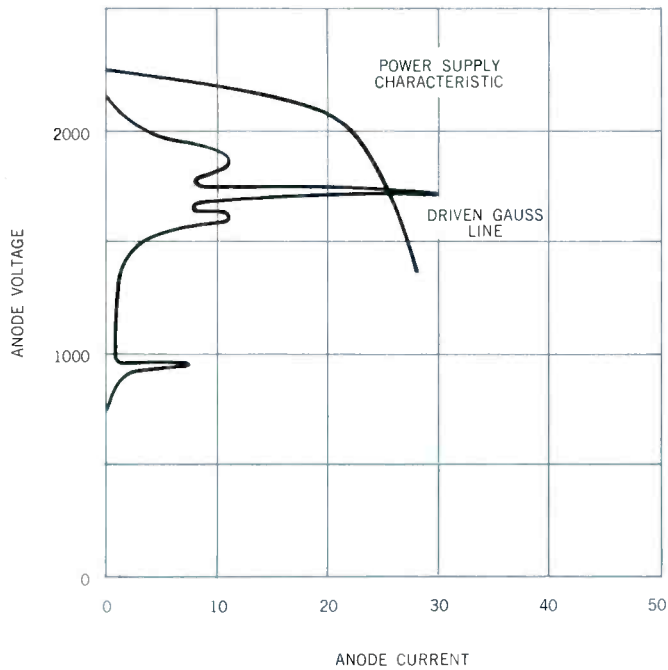


Figure 6 — QKS997A Voltage-Current Characteristics.

ply which includes current regulation, as current is a sensitive measure of proper operating voltage. The simplest form of regulator is series resistance, but this is usually rejected for all except laboratory systems because of the power lost in the dropping resistor and the relatively poor regulation provided.

The series resistor may be replaced by a vacuum tube or transistor with appreciable gain in the feedback circuit. In this case, much improved regulation is obtained with less power loss but with added complexity.

The circuit of Figure 8 has been suggested by engineers of Raytheon's Magnetics Operation and Space Information Systems Division as a means of providing low frequency regulation at high efficiency and with minimal complexity. The regulation in this case is in the primary circuit of the high voltage transformer sensing current in the secondary. It provides stabilization against input line variations as well as any changes in tube voltage arising from changes in frequency, temperature, magnetic field or the effects of life.

In the circuit shown, a similar feedback scheme is used in the heater circuit which although not imperative appears desirable from several aspects. It assures good control of the heater power by sensing the heater current. It effectively limits the surge current when power is applied to the cold heater. It provides a convenient means to introduce the reduction of heater power desired as the plate power is applied to compensate for the back bombardment heating of the cathode.

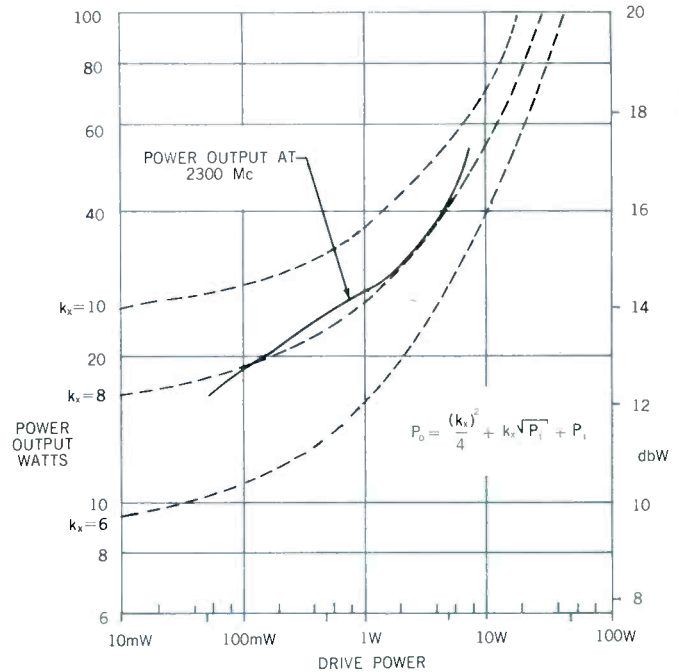


Figure 7 — Power output as a function of power input for the QKS997A with anode current adjusted for maximum at each drive power level.

As in the magnetron, some of the electrons emitted from the cathode of the Amplitron find themselves in the wrong rf phase. These accept a small amount of energy from the rf field and are driven back to the cathode. The excess energy which they have accepted from the rf field is converted to heat at the surface of the cathode. It is customary to reduce the heater power upon application of plate power to compensate for this heating effect.

These electrons striking the cathode surface also give rise to rather large amounts of secondary emission. In fact, some tubes, especially at higher powers, are operated with cathodes supplying only secondary emission. Several types of cathode operating near room temperature have been found satisfactory.

In the case of the QKS997, a conventional oxide-coated cathode with a nickel matrix developed at The Machlett Laboratories, Inc.,* has been selected. A cathode emitting area of nearly 0.4 sq. cm is provided so that primary emission densities at the 20-watt level are less than 60 mA/cm², a figure which in traveling-wave tubes is used to predict an operating life in excess of 40,000 hours. Because of the presence of back bombardment in the Amplitron emission lifetimes are expected to be somewhat less than those predicted at comparable temperatures without back bombardment.

*P. F. Varadi and K. Etre, "Simultaneous Cathaphoretic and Electrolytic Depositing Nickel for Plated Cathode of Reliable Electron Tubes," JAP.

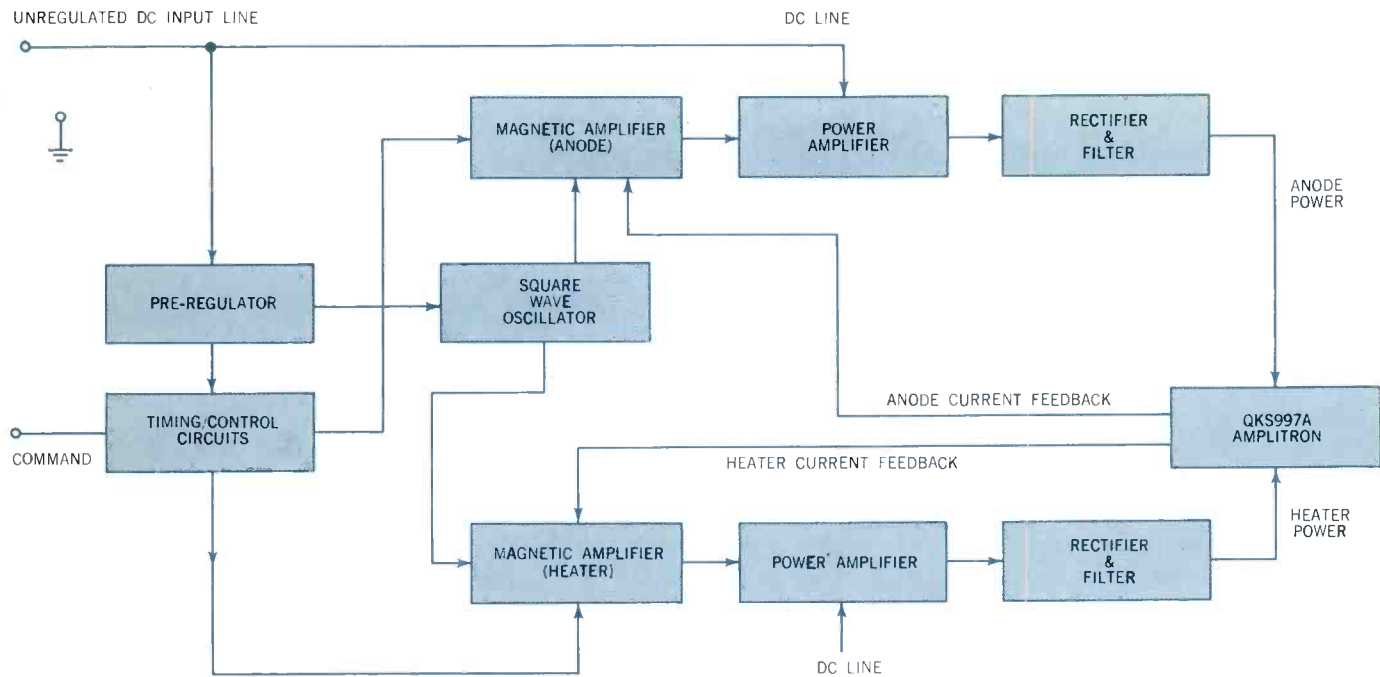


Figure 8 — Block Diagram, Amplitron Power Supply.

The space Amplitrons now being built at Spencer Laboratory are the first in which operating lifetimes greater than 10,000 hours have been the objectives of the development program. Much of the technology that has been generated by other devices has been incorporated into the Amplitron design. The validity of the translation of this technology can only be proved by extensive life tests which are currently planned.

The most critical question is, of course, the wear-out phenomenon of the cathode — to what extent can the secondary emission which is generated be used to reduce the demands for primary emission and consequently high temperatures and evaporation rates.

The ability of a cathode to supply adequate emission at low temperatures and for a long period of time is dependent on its operation in a vacuum envelope free from foreign vapors. Careful selection of materials for the vacuum envelope and advanced processing techniques including double vacuum bakeout at high temperature are employed to assure long life in the Amplitron.

The thermal design of the QKS997 is one factor which tends to reduce the possibility of gas evolution in the tube. The rf structure is designed to collect the entire electron current in normal operation. It is made up of copper parts at ground potential which provide an excellent heat path to the mounting plate. With 20 watts of dissipation, the temperature drop from the tips of the vane where electrons are collected to mounting plate is calculated to be less than 40°C.

The mechanical design of the tube is also such as to provide high resistance to damage from severe mechanical environments. Several tubes have been tested with 200g shocks in three mutually perpendicular planes without change in characteristics. Vibration tests with sinusoidal vibration at the 15g level in any of the three planes shows less than 1° rms phase modulation induced by the vibration. Data from one QKS997A is shown in Figure 9.

One of the more important characteristics with respect to frequency or phase modulated systems is the phase modulation due to power supply ripple or other sources. The relatively short electrical length of the Amplitron also contributes to a low pushing factor. The phase shift is less than 2° for a 1% change in anode current around the 20-watt operating point. Thus, a power supply with 1 volt of ripple and an internal impedance of 5000 ohms would introduce about 2° of phase shift. The phase modulation by noise is also low, less than 0.5° rms in a 500 Kc band pass. No measurable increase was found in the background of 1 to 2° in two separate systems in which a tube has been checked. An experimental tube has also been tested and found stable in a phase locked loop with a bandwidth of 20 cps.

The most serious limitation of the Amplitron for telemetry applications has been its relatively low expected gain. Most pulsed Amplitrons have been built for extremely high power operating point chosen to provide only 10 to 13 db of gain. As has been shown in the QKS997A development, however, proper selection of the operating point and good rf circuit

design can yield Amplitrons which can be operated with nearly 20 db gain. At S-band, this gain is sufficient to bring the output of a solid state exciter to the 20 to 100-watt level in a single stage.

When higher gains are required, additional Amplitron stages are practical, especially where efficient operation at several power output levels is desired. Figure 10 is a block diagram for a system in which three levels would be available — the 200-mW level of the solid state driver, the 20-watt level of the driver-Amplitron, and the 500-watt level of the final Amplitron. (The QKS1115 is currently under development.) Both of the Amplitron stages could be 60% efficient in S-band. Ferrite isolators would be included to provide non-reciprocal attenuation at least equal to the power gain. The diagram also shows two tubes for each stage to provide redundancy as has been discussed earlier.

Amplitrons are not restricted to telemetry in S-band but can be effectively scaled for operation throughout the microwave spectrum. The magnetic field required for efficient operation increases directly with frequency, and permanent magnet and pole piece materials place a practical upper limit on frequency around 100 Gc. At L-band and lower frequencies, the competition with solid-state devices will limit the applications except for fairly high powers. Units in the 100 watt to a few kilowatt range appear quite attractive at S, C and X-band and from a few watts to a few hundred watts in the higher bands. Lower power units appear to be probable at the higher frequencies to match the output power available from solid state drivers. The

upper limit on power output is a function more of spacecraft available power and of adequate cooling techniques as the basic interaction process has been shown to be capable of super-power generation.

Figure 10 — Block Diagram, 500 Watt Telemetry System with two stages at amplitron amplification and redundant tubes in each stage.

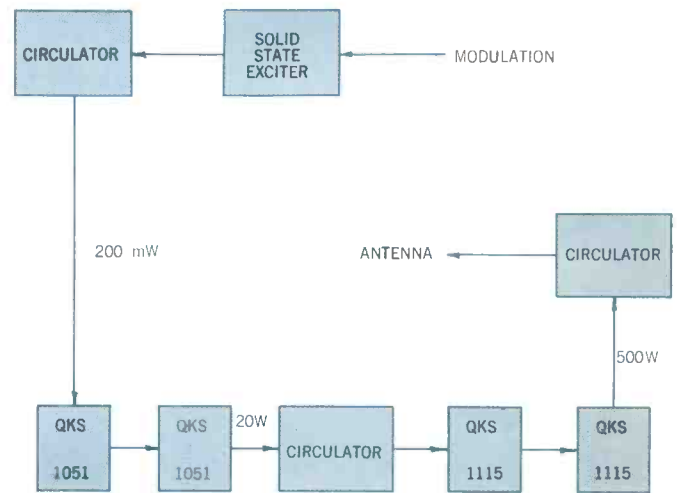
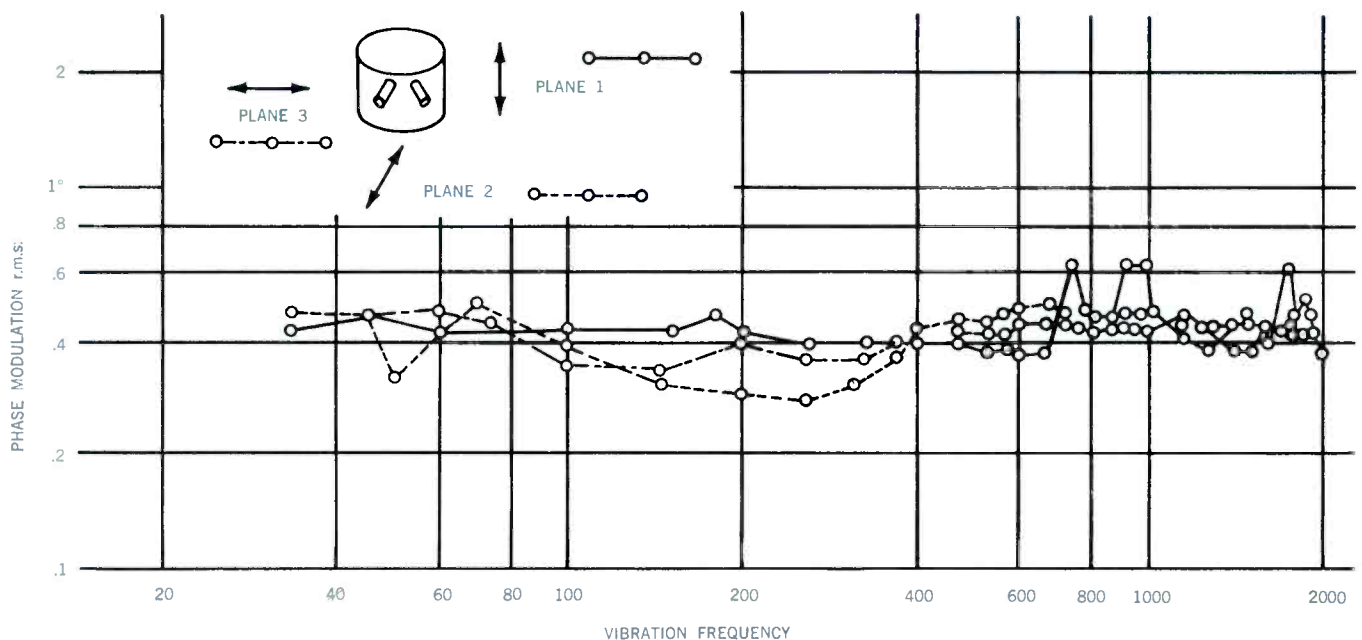
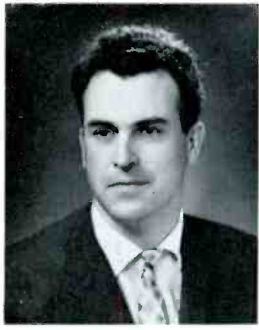


Figure 9 — Phase modulation during sinusoidal vibration, QKS997A-102 CW Amplitron, driven at 2300 Mc. Vibration level 15G at frequencies shown.





WERNER BRUNHART

Werner Brunhart joined Machlett in 1954 as a design engineer in the development of hydrogen thyratrons, pulse modulators and UHF triodes. He has been Chief Engineer, Small Power Tube Products, since 1962. Mr. Brunhart was graduated with an M.A. in Electronics from the Swiss Federal Institute of Technology in Zurich. He became an instructor there in 1951, serving the school's Advanced Electrical Engineering Department.

Negative Grid Tubes for Space Applications

By *WERNER BRUNHART, Chief Engineer, Small Power Tubes; The Machlett Laboratories, Inc.*

Introduction

The main requirements for any electron device in outer space applications is good overall efficiency, long reliable operation, a package as small and light as possible, and capability of withstanding severe environmental conditions. These requirements are not usually compatible with each other. With respect to power output and plate efficiency, the negative grid tube is only surpassed by other devices operating at higher frequencies. With respect to power gain per stage, other tubes, such as TWT's, etc., are superior to the negative grid tube. Despite this, the negative grid tube has not only been selected for space applications in the past, but also for future applications. Following are some of the advantages of the negative grid tube. No magnetic field is required which could disturb other functions in a spacecraft. Circuits employing this tube are simple and can withstand very stringent environmental requirements of up to 100 G's shock, and vibration over a wide range of frequencies up to 20 G's and more. The power supply required in conjunction with the tube does not require extensive regulation. In some cases the regulation can be omitted altogether without adversely affecting operational stability, especially with respect to frequency. The effect of nuclear radiation on tube operation is negligible.

Following are procedures which are used in the fabrication and testing of negative grid tubes which are specifically designated for space applications.

Fabrication of the Tubes

Even though tube fabrication normally requires clean and careful assembly techniques to assure a good product, it is necessary to improve these techniques still further. All ceramic parts (only metal-ceramic envelopes are used) used for these special tubes are individually inspected for cracks and chips using a microscope with a 10X magnification. In standard tube production, parts sampling is considered adequate. With special tubes, each ceramic part is again checked after metalizing for defects by backlighting. Every tenth piece is used to monitor (see Figure 1) the thickness of the metalizing (the method used is destructive). The above inspection procedure is repeated after each operation.

The metal-ceramic sub-assemblies are all radiographed for possible solder voids, and are then leak tested. In normal production, each part is checked only for leaks. However, it is felt that parts with solder voids, which are not detectable in standard tube procedures might eventually develop small leaks and require the discarding of the whole assembly.

All other tube parts receive a 100 per cent inspection, usually by engineering personnel. For instance, each grid is carefully checked for uniformity with regard to wire spacing and tension. Furthermore, each weld on the various sub-assemblies is inspected by means of a microscope. And last, but not least, the cathode assembly receives special attention to assure a clean and passive cathode emitter with uniform emitter coating.

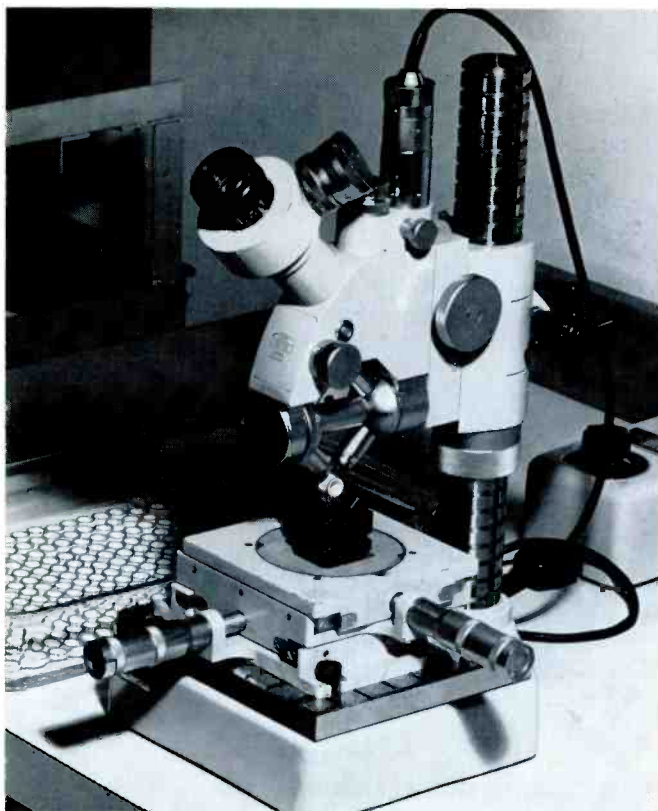


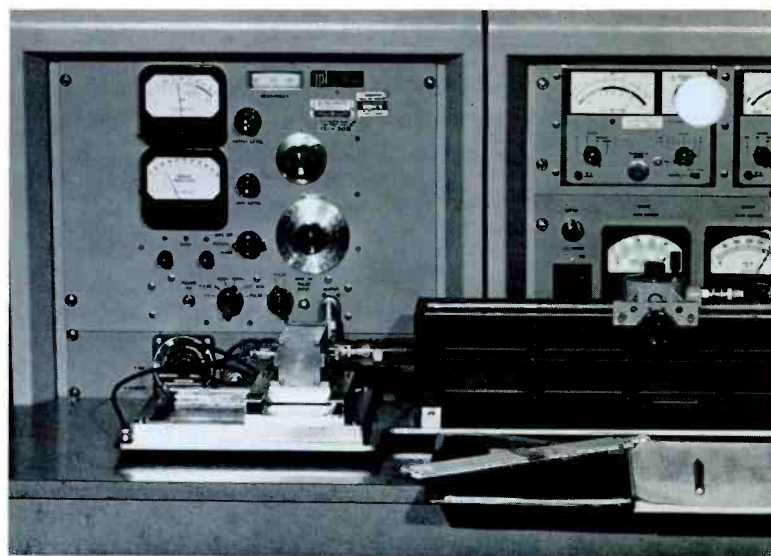
Figure 1 — Thickness of metalizing on ceramic parts are checked with specially adapted microscope.

Immediately after final assembly, all special tubes are radiographed and examined for proper location of the various elements. A leak check is performed just prior to the exhaust cycle of the multiple exhaust station to assure that no contamination takes place during this test operation.

Testing of the Tubes

After aging, the tubes are subjected to the normal static tests in order to verify that their characteristics are acceptable. Over and above these standard tests, it is mandatory that each tube be tested in the final equipment circuit under actual flight conditions (see Figures 2 and 2A). Only this test really proves if the tubes are acceptable. The test in the final equipment is repeated a second time. The first test is done only after the tubes have been shelf-aged for several days. Only tubes which repeat original test data within the accuracy of the instruments are accepted. After this the tubes receive an ambient temperature cycle of about -62°C to $+150^{\circ}\text{C}$. Then, the final test is again performed in the flight test circuit.

At this point the tubes are shipped to the user, who then conducts his own series of tests. The tubes are tested in the final circuit for at least 100 hours, during which time they are subject to shock, vibration, ambient temperature changes, etc. Only tubes which perform well and show no



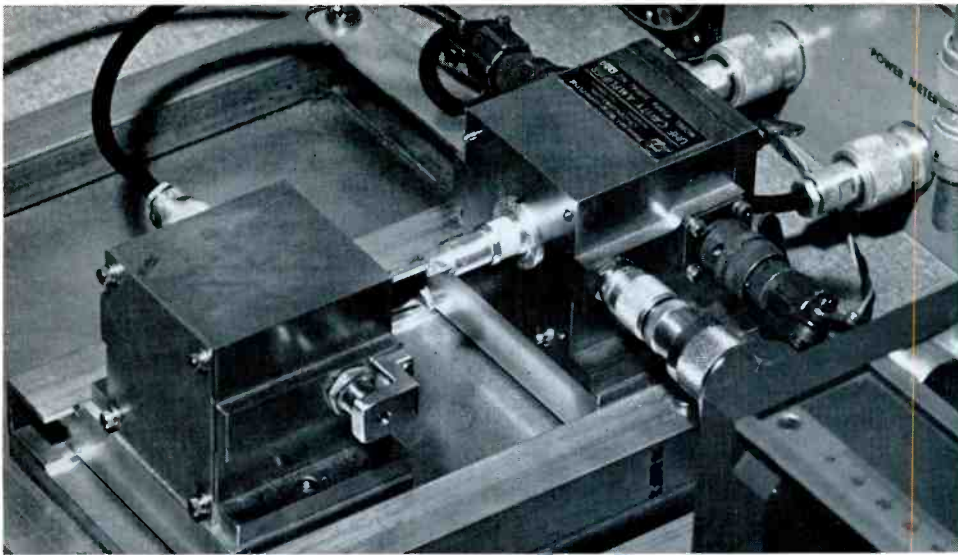
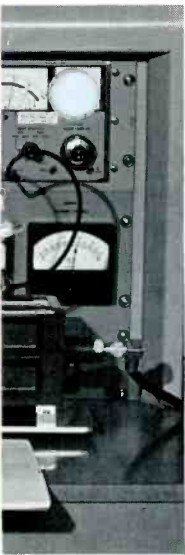
Figures 2 and 2A — Final testing of ML-6771 planar triodes for space application takes place in this power gain test set, which employs a microwave amplifier, slotted line and pre-tuned cavity. Even though this extremely precise test unit is highly stable, it is recalibrated prior to each test. At a test frequency of 960 mc, $\frac{1}{4}$ watt input, the typical output power range is 3.1 to 3.4 watts. Average VSWR readings are 1.4 to 1.45 — well below the "not-to-exceed" 1.85; readings as low as 1.1 have been made. Figure 2A shows a closer view of the Resdel amplifier cavity, preset to accept only those tubes within a narrow tuning range.

performance changes up to this point are accepted for flight equipment. In the flight equipment itself, all components undergo extensive testing which can last up to 1000 hours.

Actual Applications

To date the following tube types have been and are being used in space applications — the ML-471 (a special version of the 6442) in the Project Mercury S-Band beacon, the ML-6771 in the Project Mercury C-Band beacon, the ML-546 (a special version of the 6771) in Projects Mariner and Ranger transmitters, the ML-7855 in the TV transmitter for Project Ranger, and the ML-518 in the frequency multiplier and amplifier of Project Nimbus telemetering system. There are other applications of these tubes in various other military missiles.

Above is mentioned the importance of testing the tube in final flight circuits and conditions. This includes, of course, the filament voltage. The selection of the proper optimized filament voltage is very important. The tube life can be drastically shortened if the filament voltage is set wrong. Life tests of tubes used in Projects Mariner and Ranger indicate that the same power output can be obtained with a filament voltage of 5.2 or 5.75 volts. However the drop in power output is about 1.5 db for an amplifier chain of two tubes over a period of 15,000 hours in the first case,



and about 9.7 db in the second case; see Figures 3 and 4. This example points out the importance of the filament voltage. It also indicates that the plate power supply can be of a rather simple design and the operating conditions, (i.e., plate current and plate dissipation) have only a minor influence on the life of the tube once conditions have been optimized. At least the final amplifier tube used here is operated close to maximum ratings with respect to plate voltage and current, maximum plate power input is rated at 6.25 watts. In this application, the tube is operated at

about 5.25 watts, with a minimum power output of 3.1 watts. The current loading of the cathode in this case is approximately 150 ma/cm². It should be emphasized that no self compensating circuit was employed to automatically adjust the current for changes in the tube characteristics.

Acknowledgment

The author acknowledges with pleasure the contributions made by R. F. Spurck toward the establishment of the manufacturing and processing procedures.

Figure 3 — Power Output versus Time for ML-546 of the Pre-amplifier used in Mariner and Ranger Transmitters.

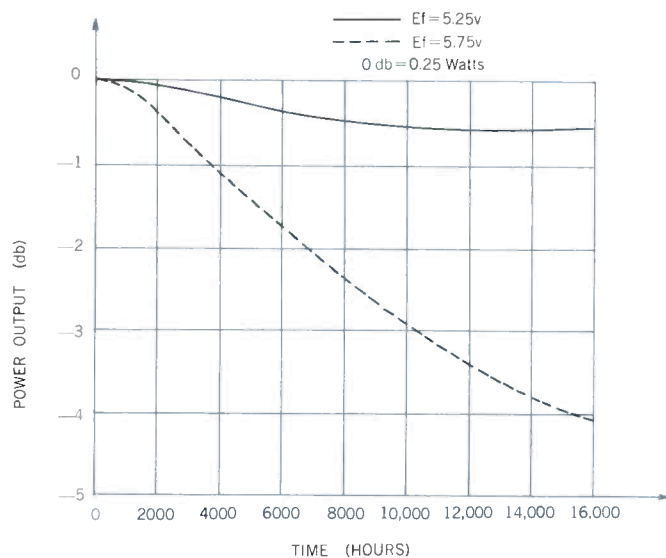
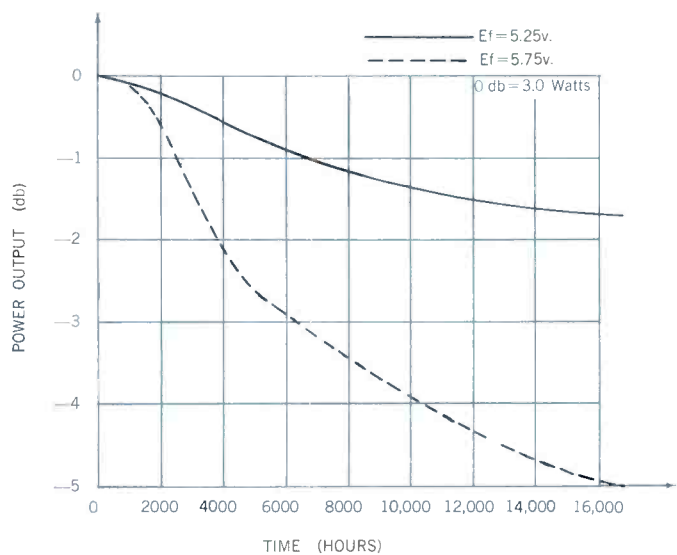
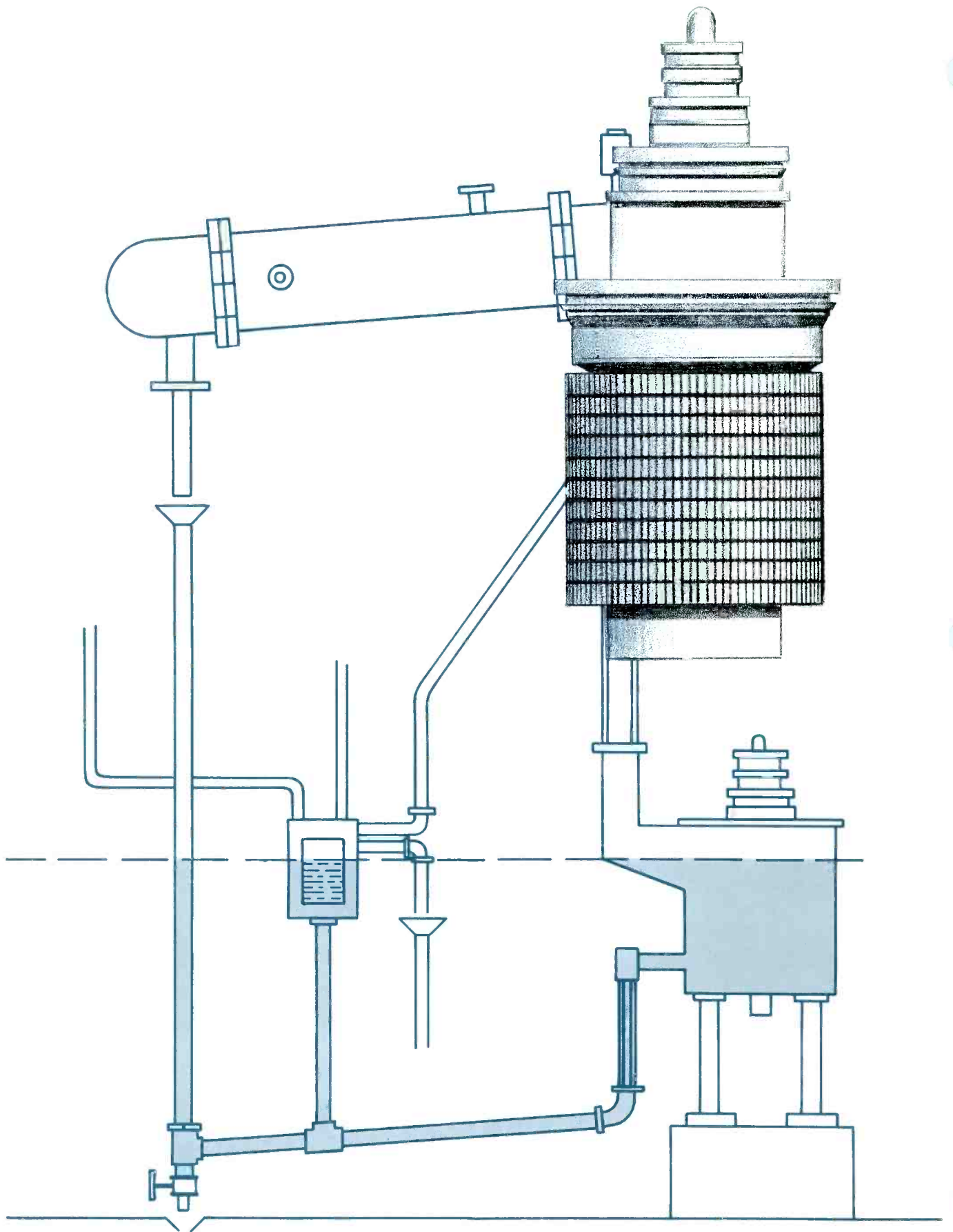


Figure 4 — Power Output versus Time for ML-546 of the Final Amplifier used in Mariner and Ranger Transmitters.





Notes on Vapor Cooling of High Power Electron Tubes

By *HELMUT LANGER, Senior Development Engineer*

and

JOSEPH FEDORCHUCK, Development Engineer

Since vapor cooling of high power electron tubes was introduced some 12 years ago, it has become a subject of increasing interest among equipment designers. Because of its inherent advantages as well as its supplementary advantages, vapor cooling has become a process proven to have superior cooling capabilities for many applications, especially those involving high power tubes. From the economic standpoint, vapor cooling is not only proving advantageous in new equipment, but it has demonstrated its value in recent conversion applications which previously employed air-cooled power tubes.

Vapor-cooling systems involve several design considerations which are not normally associated with radiation, forced-air, or forced-liquid cooling. It is the purpose of this article to outline some of these design considerations, as well as to introduce some entirely new aspects of this subject.

Heat Transfer to Boiling Liquids

Experiments on heat transfer to boiling liquids have shown that vaporization and creation of vapor bubbles often start at microscopic cavities. At a point on the anode where a vapor bubble is formed, the coefficient of heat transfer is greatly reduced until the bubble is set free. For the most part heat transfer occurs mostly at points on the anode where momentarily no vapor bubble is present. Removal of the vapor bubble is accomplished by the convection

current of the liquid, i.e., thermosyphon effect. As long as the temperature difference Δt of the anode and the liquid is relatively small, flow of the liquid and enclosed vapor bubbles stays laminar. With increasing temperature of the anode, the vapor bubbles become larger. As more bubbles are formed and are crowded in the same unit area, the vapor-liquid emulsion becomes turbulent. Figures 1, 2 and 3 are photographs illustrating bubble formation on a Machlett ML-7482 super-power triode tube at different plate dissipation levels. Maximum heat transfer in water is accomplished at Δt of approximately 25°C (see Figure 4). With increased Δt , the heat transfer rate is decreased by formation of a vapor film on the anode surface which acts as an insulator by greatly reducing the heat-transfer rate. Also, this vapor film could cause overheating and possible burn out (catafaction) between M and L (Figure 4), resulting in an overheated anode with subsequent gassing and possible tube destruction. Therefore, a change from the nucleate boiling ($\Delta t < 25^{\circ}\text{C}$) to film boiling ($\Delta t > 25^{\circ}\text{C}$) results in irreversible overheating. The maximum heat flux

$\frac{Q}{A}$ would be limited to $135\text{W}/\text{cm}^2$.

Heat Transfer in Vapor-Cooled Structures

Danger of overheating in the transition zone (M-L) (Figure 4) can be avoided when the surface of the anode

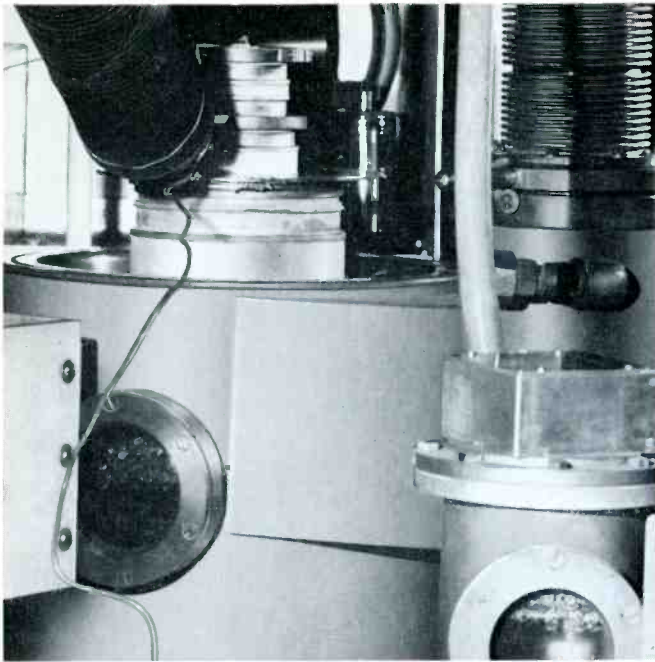


Figure 1 — ML-7482 Super Powered Triode under test in "classical" system boiler at 100 Kw plate dissipation. Note boiling action about anode visible through porthole at left.

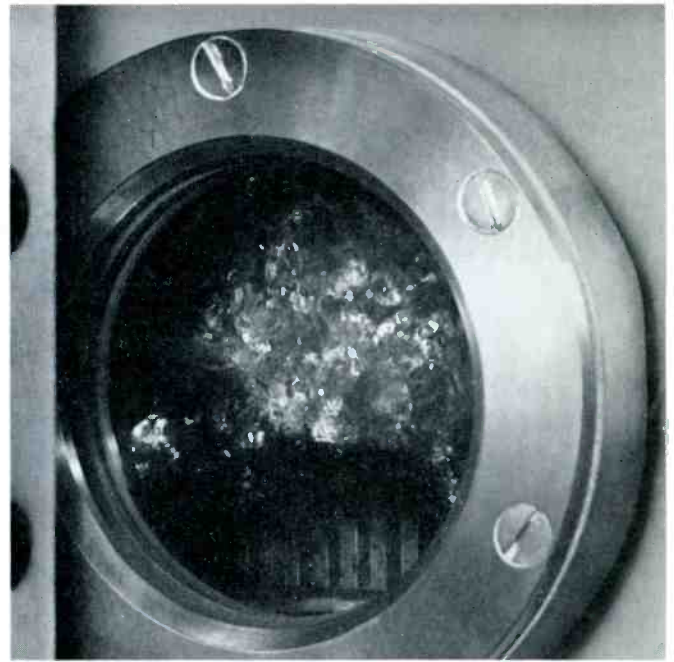


Figure 2 — Closeup of porthole shown in Figure 1 with tube operating at 150 Kw plate dissipation.

is provided with heavy protrusions, as has been developed by CFTH (France) in their early pineapple design¹. This design was later modified to a straight gear type anode design as is shown in Figure 5, probably for economic reasons. Another design which is used by Telefunken, Germany and others, utilizes a very heavy wall anode with many large holes drilled axially through the anode wall near the outer edge^{2&3}. The aforementioned anode fin tube design allows heat removal of about 200W/cm², in terms of the inner (vacuum-side) bombarded anode surface. The heat removal rate in terms of the outer corrugated surface is in the range of 35W/cm². A still later improvement developed by CFTH uses a large number of rather small, but deep radial slots. The first test results by CFTH and by Machlett indicate heat transfer capabilities of this tube in the order of >500W/cm². Figure 6 shows a Machlett ML-7482 tube with a third generation fin design, which increases plate dissipation capabilities of the anode over previous generation tubes from 200 kW to 300 kW. Safety for short time overloads is maintained.

It should be noted that radial extension within proper design configurations increases the heat dissipation of the

outer anode surface by a factor of 5 to 10. This radial extension also permits the operation of the anode in the critical transition zone without danger of burn-out. If a vapor film adheres to one local section of the fin, then heat transfer is accomplished at another section. As power dissipation is increased, more vapor bubbles are formed and more turbulence of the water-vapor emulsion is accom-

Figure 5 — ML-7482 (second generation anode fin design).
P_A = 200 Kw.



¹C. Beutheret, "The Vapotron Technique," *Review Technique*, C. F. T. H. No. 24, Paris, December 1956.

²C. Protze, "KanalKuehlung, eine Siedekuehlung von Hochleistungs HF-Generator und Senderoehren," *Telefunken Zeitung*, Vol. 29, No. 112, June 1956.

³J. Houdyshel, "Vapor Phase Cooling of High Power Equipments," *Electro Technologie*, March 1963.



Figure 3 — Closeup of porthole shown in Figure 1 with tube operating at 200 Kw plate dissipation.

plished, and thus better contact of the liquid to the anode fins takes place. Experiments have shown that so-called "twisting" of the fins (see Figure 7) on a gear type anode increases the heat transfer rate of the anode by more than 30%. At the same time, the twisted fins provide a more quiet operation from the standpoint of mechanical vibration of the tube-boiler assembly. In the earlier anode-fin designs

Figure 6 — ML-7482 (third generation anode fin design).

$P_A > 300 \text{ Kw.}$

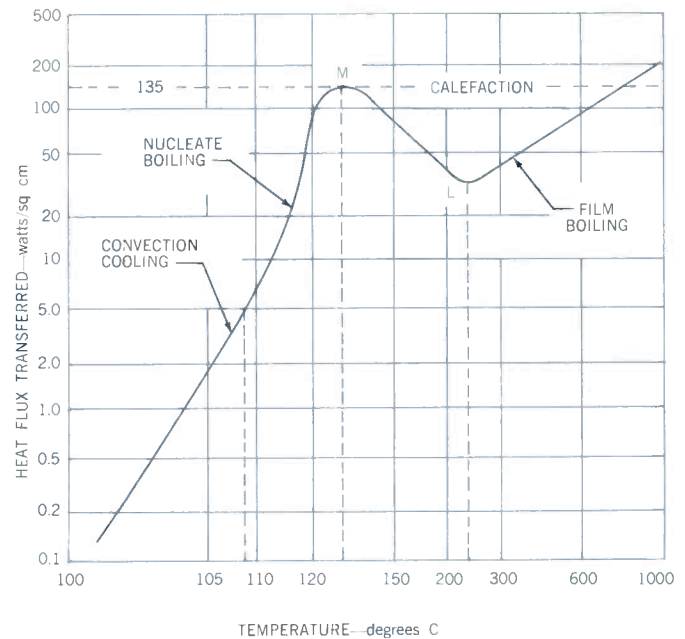
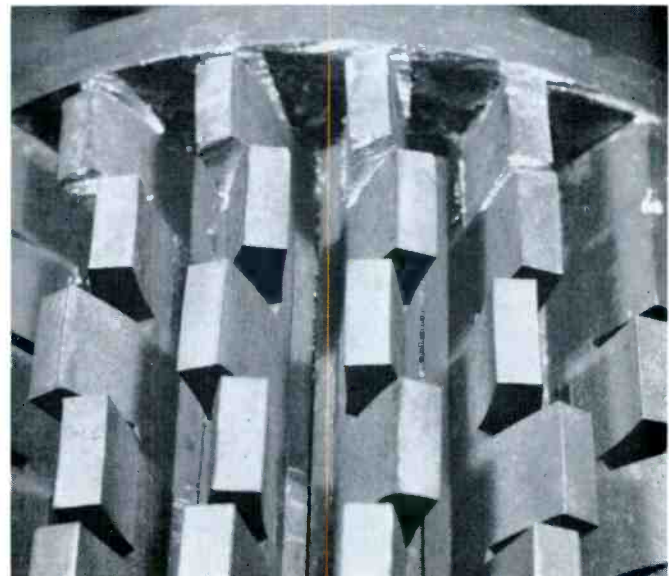


Figure 4 — Nukiyama Heat Transfer Curve For Boiling Water.

— pineapple gear type, or channel cooling type — the vapor-water emulsion was ejected at the upper opening between two fins, as directed by a rather closely surrounding jacket which creates a thermosyphon effect. In the newer fin designs with small, deep grooves (see Figure 6) vapor bubbles are free to move radially outward, forming a vapor cloud a safe distance ($1/2''$ to $1''$) away from the outer

Figure 7 — Closeup section of "twisted-fin" anode (experimental design).



external surface of the anode fin, and moving upwards towards the boiling liquid surface. One may observe this phenomena in Figure 2. Figure 8 is taken from C. A. Beutheret⁴ and shows the curve of Figure 4 in terms of

$$K = \frac{Q}{A (\Delta t)}$$

as total thermal conductance of vapor-cooled tubes with fin configurations as discussed above. Note that heat-transfer rates are increased from 150W/cm² in Curve 2 to as high as 600W/cm² in Curve 4. The transition zone C (see also Figure 4), is represented by a broken line. The efficiency curves drop rapidly when maximum thermal conductance is reached, and the structure would be subject to destruction if the power were not reduced in sufficient time. The curves in Figure 8 represent operation under steady state conditions in boiling water under atmospheric pressure.

Heat Transfer and Surface Conditions

Sufficient heat transfer under steady state conditions in vapor-cooled anode structures requires utmost care with respect to cleanliness of the boiling liquid, surface conditions of the anode structure and all system components. Generally, distilled water should be used in order to avoid sludge and scale formation on the anode surface, and to reduce the possibility of electrical breakdown in the insulated water intake due to high conductivity of the water⁵. However, clean tap-water can be used when certain precautions are taken. Clean copper in contact with the boiling liquid appears to give optimum heat transfer; slightly dirty copper can reduce heat transfer rates by 20% to 50%⁶. Oil or grease in the system will greatly reduce heat transfer and may produce carbonaceous scale deposits on the fin surface. Roughing of the anode-fin surface does not necessarily have positive effects on heat transfer. Proper acid cleaning and careful handling will, however, prevent contamination.

Aeration of the distilled water, as may be accomplished on the outlet of the heat exchanger (see Figure 10) may increase heat transfer⁷. Also, the addition of wetting agents to the distilled water may increase heat transfer by greatly reducing surface tension, thus permitting a freer escape of vapor bubbles. However, in using wetting agents, caution must be exercised to avoid scale formation.

Surface Scale Formation

The use of distilled water as the boiling liquid and the thorough rinsing of the anode fin surface by powerful turbulence greatly reduces scale formation. In a "clean" system, the anode-fin surface, after several thousand hours of op-

eration, should still only exhibit a typical brownish copper oxide appearance. This condition is established after several hours of operation under maximum power dissipation of the tube. In an initial installation frequent rinsing of the overall system, including the heat exchanger, is required to remove most of the contaminants. After a system is put into operation, it is good maintenance practice to periodically drain the system and clean the anode structure and system components. Such practice will pay dividends in reliable system performance and excellent tube life.

Application of Vapor Cooling at High Elevations

Under normal conditions, vapor-cooling of high power tubes can be used at high elevations (transmitter or radio equipments at mountain tops) without loss of efficiency in heat transfer. Figure 9 shows the decrease of heat of vaporization of water with respect to saturation temperature and elevation in feet. Heat of vaporization at 15,000 feet is decreased by 1.8%. For example, at this altitude, boiling water absorbs approximately 535 calories per gram of water vaporized as opposed to 545 calories absorbed at sea level.

Applications of vapor-cooled systems at high elevations have several distinct advantages over forced-air or forced-water cooled systems.

1. Eliminates requirement of large amounts of circulating water for forced-water systems, which is difficult to provide at high elevation transmitter locations.
2. Dissipates 200% to 300% more power than air-cooled systems.
3. Provides significant supplementary advantages: practical means of using dissipated heat for heating buildings; and, efficient means of extracting distilled water from system⁸.

Vapor Cooling at Subzero Temperatures

Many present day electron tube cooling systems must operate in remote areas under subzero temperatures. Systems using water must therefore be protected against the possibility of freezing during shutdowns or power failures. In general, water-ethylene-glycol mixtures are most frequently used (50% water-50% ethylene-glycol for approximately -40°C freezing point). For forced-water cooled and vapor-cooled systems, only purified glycol and water solutions without additives should be used⁹, as additives usually reduce the heat transfer rate. If the heat densities are high enough, local scaling may result. Machlett tests

⁴C. Beutheret, "Evaporation Process and the Vapotron."

⁵"Note on the Vapotron," Publication by the Compagnie Française Thomson-Houston, France.

⁶W. McAdams, Chapter X, "Heat Transfer to Boiling Liquids," *Heat Transmission*, McGraw-Hill, New York.

⁷Ibid.

⁸H. Langer, "Supplementary Advantages of Vapor Cooling: Space Heating and Distilled Water Production," *Cathode Press*, Vol. 20, No. 1, 1963.

⁹A. Winslow, "Coolants for High Power Radio and Transmitting Tubes," *Electronic Packaging and Production*, February 1963.

indicate that 50/50 glycol-water solutions and distilled water exhibit comparable boiling characteristics and heat transfer values. However, until sufficient field life data have been accumulated, plate dissipation values should be limited to approximately 75% of the maximum tube ratings, and rather frequent maintenance checks should be made.

With systems using glycol-water mixtures, evaporation losses on the outlet of the heat exchanger will consist mainly of water. To replenish the loss, only water has to be added. However, vapor-cooling systems normally include automatic water level controls which replenish the system from a reservoir. In most cases, it will also be necessary to maintain a glycol-water mixture in the reservoir. After a period of time, systems which initially included a 50-50 mixture, will consist of more glycol than water. It will then be necessary to institute periodic specific density tests, and if necessary replace or modify the solution to maintain the proper solution. The specific density of a 50-50 solution is 1.072g/cm³ at 60°F.

Vapor Cooling for High Frequency Applications

In conventional vapor cooling systems, the water-steam emulsion at the upper escape provides an excellent means of cooling the anode flange. This feature permits the use of a short connection between the metal tube flange and the

ceramic or glass envelope. It also reduces high frequency losses, which ultimately decrease the tube power output at high frequencies. The escaped vapor can either be discharged through an upper steam-tube, as in the Classical System (Figure 10), or it can be discharged downwards as in the Vapor-Down System (Figure 11). The latter system is of interest when considering that in high frequency applications, grounded grid operation is widely used. Discharge of the vapor downward permits tube designs with very short distances between the anode and the grid. This minimizes inductance, and subsequently increases the resonance frequency of the grid-anode circuit. While the Classical System operates without "external" power, the Vapor-Down System requires a small circulating water pump to feed the condensate back into the boiler, which is pumped at a rate 3 to 5 times more than would normally be required to compensate for losses due to vaporization. For very high frequency applications > 100Mc the Integrated High Frequency System is recommended (Figure 12). In this system the boiler becomes a part of the tube. However, the boiler-tube assembly is installed in an inverted position. The system is then operated in the same manner as the classical vapor cooling system. Advantages of this system include the reduction in size of the anode-boiler, which results in lower tube circuit capacitances that are essential in VHF installations.

Figure 8 — Conductance of Vapor Cooled Tubes.

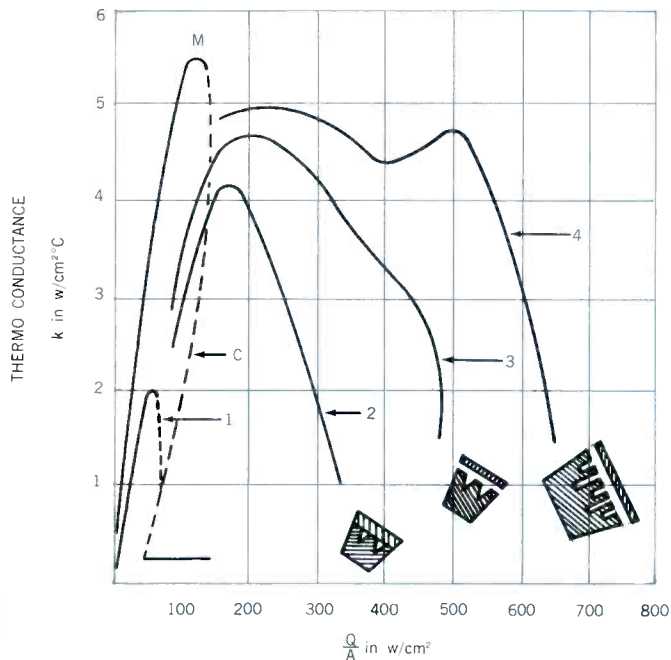
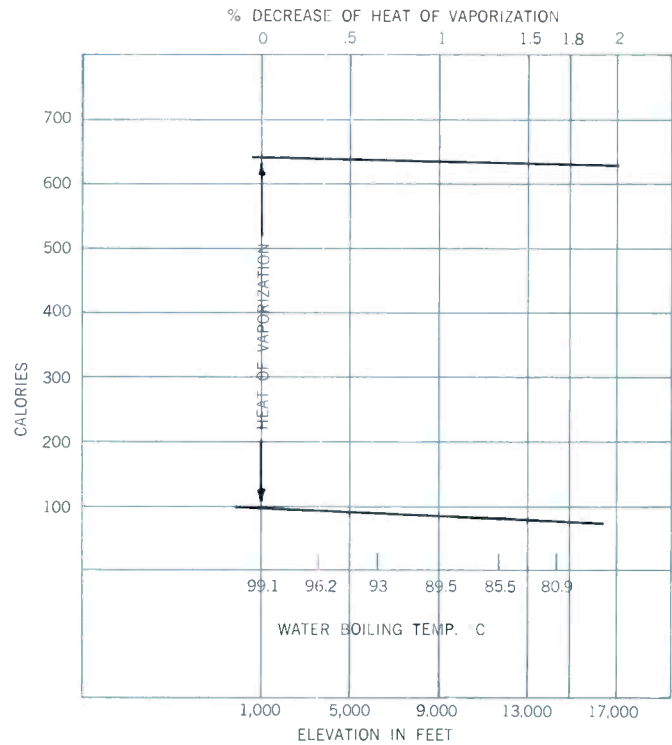


Figure 9 — Heat of Vaporization of Water versus Elevation in Feet.



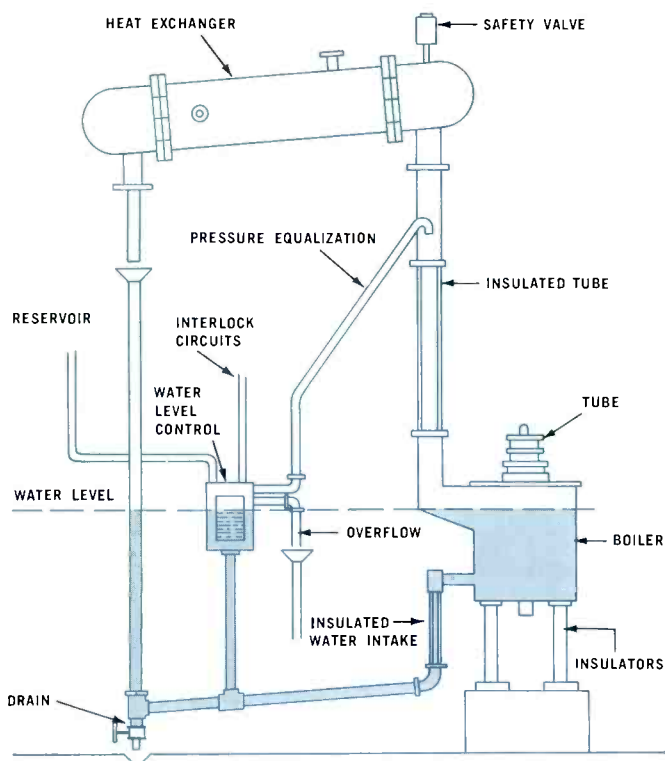


Figure 10 — Classical System. In this system the water-steam emulsion at the upper escape provides an excellent means of cooling the anode flange, permitting use of a short connection between the metal tube flange and envelope. This reduces high frequency losses which decrease the tube power output range at high frequencies.

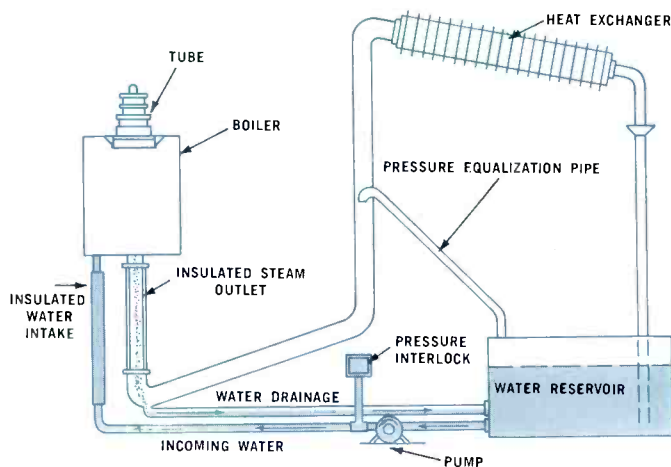


Figure 11 — Vapor-Down System. This system is to be considered for high frequency applications when grounded grid operation is used. The downward discharge of the vapor permits tube designs with very short distances between the anode and grid. This minimizes inductance, and subsequently increases the resonance frequency of the grid-anode circuit.

Economic Considerations

In any discussion of the relative merits of cooling systems for electron tubes, installation and operation costs necessarily assume a major role. In many applications the selection of vapor cooling is easily justified on costs alone¹⁰. Generally speaking, installation costs for vapor cooling systems for high power tubes are somewhat higher than air-cooled systems; installation costs are comparable with forced-water systems. However, when total operational costs are considered, cost savings in favor of vapor cooling increase with dissipation levels. For example, operating costs for 5000 hours of operation at 50 KW dissipation are approximately \$500.00 in favor of vapor cooling; and \$1000 at the 100 KW level.

Another economic factor of vapor cooling can be translated in terms of tube life. There are some indications that vapor-cooled tubes, due to maintenance of constant anode temperature, now have greater tube life expectancy than comparable air-cooled tubes.

¹⁰M. Stangl, W. Allen, "Vapor Phase Cooling of High Power Electron Tubes," *Electrical Design News*, May 1962.

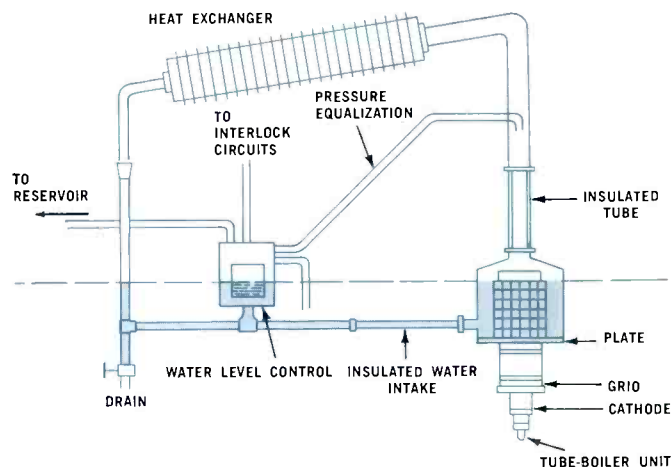


Figure 12 — Integrated High Frequency System. This system, in which the boiler is an integral part of the tube, is recommended for very high frequency applications greater than 100 Mc. Advantages of this method include the reduction in size of the anode-boiler, which results in lower tube circuit capacitances that are essential in VHF installations.

New Machlett Developments



ML-8495

High voltage triode
for
pulse modulator service
to 3 Mw

Designed to operate primarily as a switch tube in pulse modulators and other high voltage switching applications. Employs sturdy thoriated tungsten filament and integrated forced-oil-cooled anode.

Maximum Ratings Pulse Modulator or Pulse Amplifier

Plate Voltage	160 kV
Pulse Cathode Current	22 amps
Plate Dissipation	2.5 kW

Typical Operation

DC Plate Voltage	150 kV
DC Grid Voltage	-1000 v
Pulse Positive Grid Voltage	1000 v
Pulse Plate Current	18 amps
Pulse Grid Current	3 amps
Pulse Driving Power	6 kW
Pulse Power Output	2.4 Mw
Pulse Output Voltage	135 kV



ML-7482

General purpose, vapor-
cooled triode capable
of 400 kW
service at 30 Mc

New ML-7482 general purpose triode is capable of more than 400 kW continuous output as Class C amplifier or oscillator at frequencies to 30 Mc. Improved anode design dissipates up to 300 kW during momentary overloads.

Maximum Ratings as RF Power Amplifier and Oscillator Class C Telegraphy

DC Plate Voltage	20 kV
DC Grid Voltage	-1500 v
DC Plate Current	30 amps
DC Grid Current	4 amps
Plate Input	600 kW
Plate Dissipation	200 kW

Typical Operation

DC Plate Voltage	20 kV
DC Grid Voltage	-1000 v
DC Plate Current	29 amps
Driving Power, Approx.	6 kW
Power Output, Approx.	440 kW



ML-589

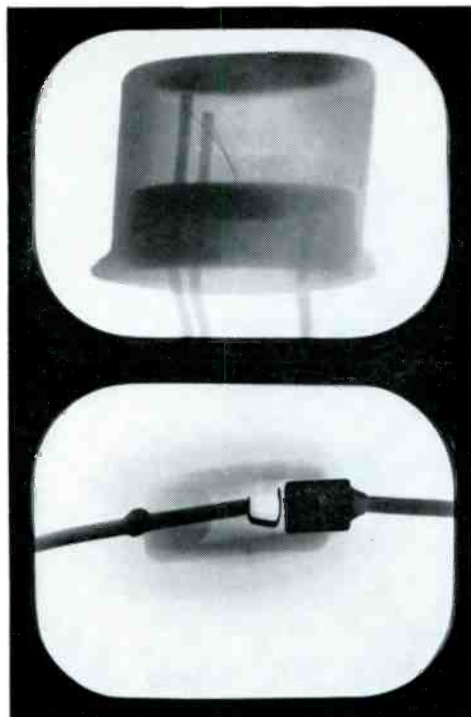
1" X-ray sensitive
vidicon for static and
in-motion
TV/x-ray systems

ML-589 "Dynamicon" provides high contrast images with detail resolution down to 0.0005", and penetrometer sensitivities up to 2%, when used with an adequate CCTV system and x-ray source. Magnification to 50X. Target current is 0.4 ua; dark current is extremely low compared with conventional light-sensitive vidicons. Especially suited for non-destructive testing and biological applications.

Typical Operating Conditions

Signal-Electrode Voltage	10 - 30 v
Grid #4 & Grid #3 Voltage	200 - 300 v
Grid #4 Voltage	300 v
Grid #1 Voltage (Picture Cut-off)	45 to 100 v
Highlight Signal- output Current	0.05 - 0.2 ua
Visual Equiv. Signal to Noise Ratio, Approx.	300:1

X-Ray Vidicon



X-ray TV image of metal-clad transistor and encapsulated diode—a typical non-destructive testing application.



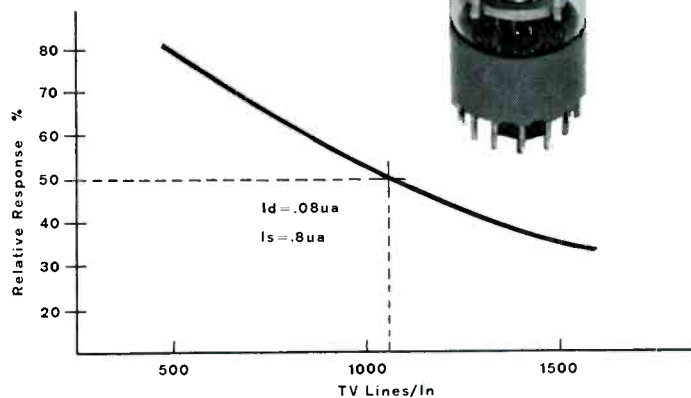
High quality—static and in-motion— X-ray TV images . . .

The New ML-589 DYNAMICON is a 1" x-ray-sensitive vidicon camera tube which is capable of providing high contrast images with detail resolution down to 0.0005", and penetrometer sensitivities up to 2%, when used with an adequate CCTV system and x-ray source. Magnifications to 50X are easily obtainable. ML-589 is particularly suited for non-destructive testing and biological applications, permitting both static and in-motion examinations of small encapsulated components and materials such as plastics, ceramics, steel, aluminum, and rubber.

For complete details write
The Machlett Laboratories,
Inc., Springdale, Conn. An
affiliate of Raytheon Co.



2" Vidicon



Only one vidicon has resolution exceeding 2000 TV lines

The new ML-2058G 2-inch diameter TV pickup vidicon is the only vidicon that provides this high detail resolution. Features of the ML-2058G include: 1.4" diagonal working area; a limiting resolution exceeding 2000 TV lines; 50% amplitude modulation at 1100 TV lines. It is designed for operation with conventional image orthicon deflection coils. Length is 12". Available with x-ray sensitive photoconductor. For complete details write The Machlett Laboratories, Inc., Springdale, Conn. An affiliate of Raytheon Co.



**THREE COOLING OPTIONS IN
HIGH POWER COAXIAL TRIODES**



**FORCED AIR COOLING
ML-8317**

Typical power capabilities:
SSB 100 kW (2 tone)
Plate Mod. RF 125 kW
Pulse Mod. 15 Mw
Max. Anode dissip. 60 kW



**VAPOR COOLING
ML-7482**

Typical power capabilities:
CW 400 kW
SSB 230 kW (2 tone)
Plate Mod. RF 250 kW
Max. Anode dissip. 200 kW



**WATER COOLING
ML-7560**

Typical power capabilities:
CW 400 kW
Pulse RF 2.5 Mw
Pulse Mod. 15 Mw
Max. Anode dissip. 175 kW

ALL THREE COOLING OPTIONS use basic, proven electron tube structure: Coaxial, easily cooled terminals; ceramic insulation; thoriated tungsten cathode; heavy wall anode. For technical data write: The Machlett Laboratories, Inc., Springdale, Conn. An affiliate of Raytheon Company.

